Research Paper

PAIN®

OPEN

The T-type calcium channel $Ca_V3.2$ regulates bladder afferent responses to mechanical stimuli

Luke Grundy[a,b,c,*], Cindy Tay[a,b], Stewart Christie[d], Andrea M. Harrington[a,b], Joel Castro[a,b], Fernanda C. Cardoso[e], Richard J. Lewis[e], Vladimir Zagorodnyuk[d], Stuart M. Brierley[a,b,c]

Abstract

The bladder wall is innervated by a complex network of afferent nerves that detect bladder stretch during filling. Sensory signals, generated in response to distension, are relayed to the spinal cord and brain to evoke physiological and painful sensations and regulate urine storage and voiding. Hyperexcitability of these sensory pathways is a key component in the development of chronic bladder hypersensitivity disorders including interstitial cystitis/bladder pain syndrome and overactive bladder syndrome. Despite this, the full array of ion channels that regulate bladder afferent responses to mechanical stimuli have yet to be determined. Here, we investigated the role of low-voltage-activated T-type calcium (Ca_V3) channels in regulating bladder afferent responses to distension. Using single-cell reverse-transcription polymerase chain reaction and immunofluorescence, we revealed ubiquitous expression of $Ca_V3.2$, but not $Ca_V3.1$ or $Ca_V3.3$, in individual bladder-innervating dorsal root ganglia neurons. Pharmacological inhibition of $Ca_V3.2$ with TTA-A2 and ABT-639, selective blockers of T-type calcium channels, dose-dependently attenuated ex-vivo bladder afferent responses to distension in the absence of changes to muscle compliance. Further evaluation revealed that $Ca_V3.2$ blockers significantly inhibited both low- and high-threshold afferents, decreasing peak responses to distension, and delayed activation thresholds, thereby attenuating bladder afferent responses to both physiological and noxious distension. Nocifensive visceromotor responses to noxious bladder distension in vivo were also significantly reduced by inhibition of Ca_V3 with TTA-A2. Together, these data provide evidence of a major role for $Ca_V3.2$ in regulating bladder afferent responses to bladder distension and nociceptive signalling to the spinal cord.

Keywords: Bladder, Afferent, Distension, $Ca_V3.2$, Nociception, Pain

1. Introduction

Bladder sensation depends on the activation of sensory afferent nerves embedded within the bladder wall.[19] Sensory signals are generated during bladder distension and transmitted to the dorsal horn of the spinal cord, feeding into spinal reflex and cortical pathways that modulate autonomic bladder function and conscious bladder sensation.[22,35] Hyperexcitability of these sensory afferent pathways is fundamental to the development of the urinary urgency, frequency, and pain that defines chronic bladder hypersensitivity disorders such as interstitial cystitis/bladder pain syndrome (IC/BPS) and overactive bladder syndrome (OAB).[20,28]

The transduction of bladder stretch into a sensory signal destined for the CNS relies on the coordinated activity of multiple mechanosensitive and nonmechanosensitive ion channels.[27,51,53,76] Mechanosensitive ion channels are necessary for the initial transduction of mechanical distortion of the bladder wall into electrochemical signals.[1,53,76] However, the final sensory signals that are sent to the CNS are shaped by the presence of multiple voltage-gated ion channels that regulate the excitability of sensory nerves.

Low-voltage-activated T-type calcium channels (Ca_V3) are well-known regulators of neuronal excitability and neuronal communication.[84] Three subtypes of Ca_V3 channels exist: $Ca_V3.1$, $Ca_V3.2$, and $Ca_V3.3$. Overall, $Ca_V3.2$ is the predominant channel expressed in both the peripheral and the central endings of primary afferent neurons,[61,67,75,85] and its activity regulates the transmission of painful stimuli in both physiological and pathological states.[7] Pharmacological inhibition, genetic knock-out, or downregulation of $Ca_V3.2$ reduces neuronal excitability ex vivo and attenuates pain responses in animal models of inflammatory, neuropathic, and visceral pain in vivo.[6,13,14,23,24,62,67,78] Correspondingly, selective activation of $Ca_V3.2$ induces neuronal hyperexcitability, and upregulation of $Ca_V3.2$ in peripheral sensory structures is observed in chronic pain states associated with afferent

Sponsorships or competing interests that may be relevant to content are disclosed at the end of this article.

[a] *Visceral Pain Research Group, College of Medicine and Public Health, Flinders Health and Medical Research Institute (FHMRI), Flinders University, Bedford Park, Australia,* [b] *Hopwood Centre for Neurobiology, Lifelong Health Theme, South Australian Health and Medical Research Institute (SAHMRI), Adelaide, Australia,* [c] *Discipline of Medicine, University of Adelaide, Adelaide, Australia,* [d] *Human Physiology, Flinders Health and Medical Research Institute (FHMRI), Flinders University, Bedford Park, Australia,* [e] *Institute for Molecular Bioscience, The University of Queensland, St. Lucia, Australia*

**Corresponding author. Address: Visceral Pain Research Group, Level 7, South Australian Health and Medical Research Institute (SAHMRI), North Terrace, SA 5000, Australia. Tel.: +61 8 8128 4858. E-mail address: luke.grundy@flinders.edu.au (L. Grundy).*

Supplemental digital content is available for this article. Direct URL citations appear in the printed text and are provided in the HTML and PDF versions of this article on the journal's Web site (www.painjournalonline.com).

PAIN 164 (2023) 1012–1026

http://dx.doi.org/10.1097/j.pain.0000000000002795

hypersensitivity.[16,26,44,46,52,73] Accumulating evidence suggests that alterations in sensation during modulation of $Ca_V3.2$ may reflect a key role for $Ca_V3.2$ in amplifying mechanoreceptor signals in the peripheral endings of primary afferent neurons.[24,38,78]

Increased $Ca_V3.2$ activity has also been implicated in bladder pathophysiology, regulating bladder overactivity in chronic bladder outlet obstruction and referred pelvic pain of the abdomen during chemical induced cystitis.[42,54,60] Despite this, the mechanisms and anatomical structures that regulate $Ca_V3.2$ modulation of bladder function have yet to be explored. We recently reported that combined inhibition of voltage-gated sodium channels and T-type calcium channels inhibited the sensitivity of peripheral sensory neurons innervating the bladder to distension.[11] However, inhibition of voltage-gated sodium channels alone exerts dramatic inhibition of bladder afferent excitability.[34] As such, whether Ca_V3 channels independently regulate bladder afferent responses to mechanical distension has not been thoroughly explored or reported upon.

In this study, we addressed this significant knowledge gap. Using single-cell reverse-transcription polymerase chain reaction (RT-PCR), we identified ubiquitous expression of $Ca_V3.2$, but not $Ca_V3.1$ or $Ca_V3.3$, in the cell bodies of bladder-innervating sensory neurons. Pharmacological inhibition of $Ca_V3.2$ with TTA-A2 and ABT-639 significantly reduced bladder afferent responses to distension ex vivo, and TTA-A2 reduced nocifensive responses to bladder distension in vivo. Low- and high-threshold bladder afferents were inhibited by TTA-A2 and ABT-639, displaying reduced peak firing and delayed activation thresholds to distension. Together, these data provide evidence for a major role for $Ca_V3.2$ in regulating bladder afferent responses to mechanical stimuli.

2. Methods

2.1. Ethics and animals

In this study, 12- to 18-week-old male and female C57BL/6J mice (JAX strain #000664) were used from an in-house breeding colony at the South Australian Health and Medical Research Institute (SAHMRI). Mice were originally purchased from The Jackson Laboratory (breeding barn MP14; Bar Harbor, ME) and then bred within the specific and opportunistic pathogen-free animal care facility at SAHMRI. These studies also used a $Na_V1.8$Cre-TdTomato mouse. Transgenic mice on a C57Bl/6 background expressing Cre recombinase under control of the $Na_V1.8$ promoter were generously donated by A/Prof Wendy Imlach (Monash University, Melbourne, Australia). $Na_V1.8$-Cre mice were crossed with tdTomato (donated by Dr Jia Ng at SAHMRI, Adelaide, Australia) reporter mice; these mice possess a loxP-flanked Stop cassette that is excised in Cre-expressing neurons, allowing tdTomato production in cells expressing $Na_V1.8$Cre only. All mice were group housed (up to 5 mice per cage) within individual ventilated cages filled with chip coarse dust-free aspen bedding (PuraChips Aspen coarse 63L; Cat# ASPJMAEB-CA; Able Scientific, Perth, Australia), with free access to LabDiet JL Rat and Mouse/Auto6F chow (Speciality Feeds, Australia) and autoclaved reverse osmosis water. Cages were stored within a temperature-controlled environment of 22°C and a 12-hour light/12-hour dark cycle on individual ventilated cage racks. Female guinea pigs (373 ± 11 g) were obtained from the Flinders University Animal facility and maintained under 12-hour light/dark cycles with ad libitum access to food and water. All animal care and experimental procedures were approved by the Animal Welfare Committee of Flinders University (ID: 1574-5) or SAHMRI animal ethics committee (SAM#195) and performed in accordance with the Australian code of practice for the care and use of animals for scientific purposes (Eighth Edition, 2013, National Health and Medical Research Council of Australia) and the Animals in Research: Reporting in vivo Experiments guidelines.[47] Experiment sample sizes are detailed in the corresponding figure legends.

2.2. Ex vivo bladder afferent nerve recordings

Nerve recordings were performed using a previously described ex vivo model in female (N = 10) and male (N = 5) mice.[29,32,35] Mice were humanely killed via CO_2 inhalation, and the entire lower abdomen was removed and submerged in a modified organ bath under continual perfusion with gassed (95% O_2 and 5% CO_2) Krebs-bicarbonate solution (composition in mmol/L: 118.4 NaCl, 24.9 $NaHCO_3$, 1.9 $CaCl_2$, 1.2 $MgSO_4$, 4.7 KCl, 1.2 KH_2PO_4, and 11.7 glucose) at 35°C. The bladder, urethra, and ureters were exposed by removing excess tissue. Ureters were tied with 4-0 perma-hand silk (Ethicon, Raritan, NJ, #LA53G). The bladder was catheterised (PE 50 tubing) through the urethra and connected to a syringe pump (NE-1000) to allow a controlled fill rate of 100 μL/minute with saline (NaCl, 0.9%). A second catheter was inserted through the dome of the bladder, secured with silk, and connected to a pressure transducer (NL108T2; Digitimer, Welwyn Garden City, United Kingdom) to enable intravesical pressure recording during graded distension. Pelvic nerves, isolated from all other nerve fibres between the pelvic ganglia and the spinal cord, were dissected into fine multiunit branches, and a single branch was placed within a sealed glass pipette containing a microelectrode (WPI) attached to a Neurolog headstage (NL100AK; Digitimer). Nerve activity was amplified (NL104), filtered (NL 125/126, bandpass 50-5000 Hz, Neurolog; Digitimer), and digitised (CED 1401; Cambridge Electronic Design, Cambridge, United Kingdom) to a PC for offline analysis using Spike2 software (Cambridge Electronic Design). The number of action potentials crossing a preset threshold at twice the background electrical noise was determined per second to quantify the afferent response. Single-unit analysis was performed offline by matching individual spike waveforms through linear interpolation using Spike2 version 5.18 software.

Single afferent units were characterised as previously described.[8,31,35] Afferent units were deemed "low threshold" if continuous action potential firing was elicited at less than 16 mm Hg. By contrast, "high-threshold" afferents displayed continuous action potential firing only when pressures exceed 16 mm Hg. Based on these criteria, 128 single units were identified across 15 individual experiments. In total, 30 of 128 single units were classified as "high threshold" and 98 of 128 were classified as "low threshold."

2.2.1. Afferent recording experimental protocols

At the start of each afferent recording experiment, control bladder distensions were performed with intravesical infusion of saline (NaCl, 0.9%) at a rate of 100 μL/minute to a maximum pressure of 50 mm Hg at 10-minute intervals to assess the viability of the preparation and reproducibility of the intravesical pressure and neuronal responses to distension. The volume in the bladder was extrapolated from the known fill rate (100 μL/minute) and the time taken (seconds) to reach a specific pressure. Compliance was determined by plotting intravesical pressure against the calculated volume. After a stable baseline was maintained, the saline in

the infusion pump was replaced with TTA-A2 (N = 5 male mice and N = 5 female mice; 10-100 μM; Alomone labs, Jerusalem, Israel; Cat #: T-140) dissolved in dH_2O to form stock solutions at 10 mM or ABT-639 (N = 5 female mice; 100 μM; Tocris Cat # 6770) dissolved in DMSO to form stock solutions at 20 mM that were frozen at −80°C and defrosted immediately before being used for each experiment. The single nerve bundle isolated and inserted into the glass electrode during the dissection process was contained within the recording electrode for the entire experiment, allowing comparisons between afferent firing rates to be compared in the same nerve fibres before and after intrabladder incubation with ABT-639 or increasing doses of TTA-A2. ABT-639 is a peripherally acting, selective T-type Ca^{2+} channel blocker that exhibits little or no activity at other ion channels and receptors.[45] TTA-A2 is a potent, state-dependent, and highly selective T-type Ca_V antagonist that inhibits all 3 subtypes of low-voltage-gated T-type channels ($Ca_V3.1$, $Ca_V3.2$, and $Ca_V3.3$) with comparable potencies.[50,64]

2.3. mRNA expression analysis in whole dorsal root ganglia

2.3.1. Dorsal root ganglia and brain isolation

Sixteen- to eighteen-week-old male (N = 4) and female (N = 4) mice were humanely euthanised via CO_2 inhalation, and the bladder and lumbosacral (L5 through S1) dorsal root ganglia (DRG) were removed. Brain and brain stem were removed from male (N = 4) mice for use as a positive control for Ca_v3 primers. Dorsal root ganglia and brain were frozen in liquid nitrogen and stored at −80°C for RNA extraction and quantitative reverse-transcription polymerase chain reaction (qRT-PCR) as per previous published protocols.[12,29,34]

2.3.2. RNA extraction

RNA from whole DRG and brain was extracted using the PureLink RNA Micro kit (Invitrogen, Victoria, Australia, #12183-016) with DNAse treatment (Life Technologies, Carlsbad, CA, #12185-010) according to the manufacturer's instructions. A NanoDrop Lite spectrophotometer (Thermofisher Scientific, Waltham, MA) was used to determine RNA purity and quantity. Using SuperScript VILO Master Mix (Invitrogen, #11755250), RNA was reverse transcribed to cDNA as per the manufacturer's instructions. cDNA was then stored at −20°C for QRT-PCR.[12,34]

2.3.3. Quantitative reverse-transcription polymerase chain reaction

Quantitative reverse-transcription polymerase chain reaction was performed using Taqman Gene Expression Master Mix (Applied Biosystems, Victoria, Australia, #4369016) with commercially available hydrolysis probes (TaqMan; Life Technologies; see **Table 1** for details) and RNAse-free water (AMBION, Victoria, Australia; #AM9916). For each reaction, 10 μL of qPCR MasterMix, 1 μL of TaqMan primer assay, 4 μL of water, and 5 μL of cDNA (1:2 dilution in RNA-free H_2O) from each sample was tested in duplicate for each target. Endogenous controls Actb (β-actin) and Hprt (glyceraldehyde 3-phosphate dehydrogenase and hypoxanthine phosphoribosyltransferase) were used for DRG and brain. Assays were run for 45 cycles on a 7500 Fast Real-Time PCR System (Applied Biosystems) machine, using 7500 Fast software, v2.0.6. mRNA quantities are expressed as $2^{-\Delta Ct}$ relative to reference gene *Actb x Hprt* (geometric mean).[12,29,30,34]

2.4. Retrograde tracing from the bladder

Retrograde neuronal tracing was performed as previously described.[12,29,30,34] A small, aseptic, abdominal incision was made in anaesthetised (2%-4% isoflurane in oxygen) male and female mice. A 5-μL Hamilton syringe attached to a 30-gauge needle was used to inject cholera toxin subunit B conjugated to AlexaFluor 488 (CTB-488, 0.5% diluted in 0.1 M phosphate buffered saline [PBS] pH 7.4; ThermoFisher Scientific) at 3 sites into the bladder wall (3 μL per injection).[29,30] To prevent injection of CTB into the bladder lumen, the needle was inserted subserosally, parallel with the bladder muscle. The abdominal incision was then sutured closed, and analgesic (Buprenorphine [Temvet]; 0.1 mg/kg; Troy Laboratories Pty Ltd, Glendenning, Australia; APVMA #67612) and antibiotic (Amoxicillin; 50 mg/kg; Amoxil; AUSTR11137) were administered subcutaneously as mice regained consciousness. After laparotomy, mice were individually housed and allowed to recover. After 4 days, mice were humanely euthanised by CO_2 asphyxiation, and the lumbosacral (LS; L5 through S1) DRG were removed for subsequent isolation and culture of the neurons to visualise CTB-labelled bladder-innervating neurons among the DRG neurons.[35]

2.5. Cell culture of bladder-innervating dorsal root ganglia neurons

Four days after retrograde tracing, mice were humanely euthanised via CO_2 inhalation, and lumbosacral (LS; L5 through S1) DRG were removed. Dorsal root ganglia were digested in Hanks balanced salt solution (HBSS; pH 7.4; Life Technologies, #14170161) containing 3 mg/mL collagenase II (GIBCO, ThermoFisher Scientific, #17101015) and 4 mg/mL dispase (GIBCO, ThermoFisher Scientific, #17105041) at 37°C for 30 minutes. After aspiration of the collagenase-dispase solution, DRG were incubated in HBSS containing collagenase (3 mg/mL) only for 10 minutes at 37°C. After subsequent washes in HBSS, trituration through fire-polished Pasteur pipettes of descending diameter in 600 μL complete Dulbecco's Modified Eagle Media (DMEM [GIBCO, ThermoFisher Scientific, #11995065]; 10% foetal calf serum [Invitrogen, ThermoFisher Scientific, MA]; 2 mM L-glutamine [GIBCO, ThermoFisher Scientific, #25030081], 100 μM MEM nonessential amino acids [GIBCO, ThermoFisher Scientific, #11140076], 100 mg/mL penicillin/streptomycin [GIBCO, ThermoFisher Scientific, #15070063], and 96 μg/L nerve growth factor-7S [Sigma, Victoria, Australia, N0513-0.1 MG]) mechanically disrupted DRG and dissociated cells, which were then centrifuged for 1 minute at 50*g*. Supernatant was gently aspirated, and neurons were resuspended in 360 μL of complete DMEM and spot-plated (30 μL) onto laminin-coated (20 μg/mL; Sigma-Aldrich, Victoria, Australia, #L2020) and poly-D-lysine–coated (800 μg/mL; ThermoFisher Scientific) 13-mm coverslips. Coverslips were incubated for 2 to 3 hours at 37°C in 5% CO_2 to allow adherence of neurons before flooding with 2 mL of complete DMEM. Cultured neurons were then maintained in an incubator at 37°C in 5% CO_2 for 24 hours for calcium imaging and immunohistochemistry or 4 hours for cell picking for single-cell RT-PCR.[29,30]

2.6. Single-cell reverse-transcription polymerase chain reaction of individual bladder-innervating dorsal root ganglia neurons

Single-cell RT-PCR was performed as previously described[12,29,30,34] using single neurons picked from both male

Table 1

Primers used in quantitative reverse-transcription polymerase chain reaction and single-cell polymerase chain reaction.

Gene alias	Gene target	Assay ID
β-Actin (reference gene)	Actb	Mm00607939_s1
HRPT (reference gene)	Hprt	Mm03024075_m1
Calcium voltage-gated channel subunit alpha1 G ($Ca_v3.1$)	Cacna1g	Mm01299131_m1
Calcium voltage-gated channel subunit alpha1 H ($Ca_v3.2$)	Cacna1h	Mm00445382_m1
Calcium voltage-gated channel subunit alpha1 I ($Ca_v3.3$)	Cacna1i	Mm01299033_m1
Transient receptor potential vanilloid 1	Trpv1	Mm01246300_m1
5-Hydroxytryptamine (serotonin) receptor 3A	Htr3a	Mm00442874 m1
Purinergic receptor P2X, ligand-gated ion channel, 3	P2rx3	Mm00523699_m1
Tubulin, beta 3 class III (neuronal marker)	Tubb3	Mm00727586 m1

(N = 4) and female (N = 4) mice. Under continuous perfusion of sterile and RNA-/DNase-free PBS, single retrogradely traced bladder DRG neurons were identified using a fluorescence microscope and collected into the end of a fine glass capillary using a micromanipulator.[29,30] Glass capillaries were pulled on a P-97 micropipette puller (Sutter Instruments, Novato, CA) so that the end of the pipette was equal to the diameter of an average sized cell body. The glass capillary containing the cell was then broken into a sterile Eppendorf tube containing 10 μL of lysis buffer with DNAse (TaqMan Gene Expression Cells-to-CT Kit; Invitrogen, #4399002). A bath control was also taken for each coverslip and analysed concurrently. After lysis and DNAse treatment, samples were immediately frozen on dry ice and stored at −80°C until cDNA synthesis was performed. RNA was reverse transcribed to cDNA using SuperScript IV VILO Master Mix with ezDNase Enzyme (Invitrogen, #11766500) as per the manufacturer's instructions. cDNA was then stored at −20°C for real-time PCR. Tubulin-3 expression was used as a neuronal marker and positive control. Expression of each target gene within a single cell was determined by looking at the log (ΔRn) curve against cycle number. Expression was considered positive if a complete curve was observed before 50 cycles.

2.7. Calcium imaging of cultured dorsal root ganglia neurons

Cultured DRG neurons (18-48 hours) from both male (N = 4) and female (N = 4) mice were loaded with 2.5 μM Fura-2-acetoxymethyl ester (Fura-2; Invitrogen, ThermoFisher Scientific, #F1221) in 0.01% pluronic F-127 (Invitrogen, ThermoFisher Scientific, #P3000MP) at 37°C for 30 minutes followed by a 10-minute wash with HEPES buffer (10 mM HEPES sodium salt [4-(2-hydroxyethyl)piperazine-1-ethanesulfonic acid sodium salt; Sigma, #H7006-100 G], 140 mM NaCl [Chem Supply, #SA046-3KG], 4 mM KCl [Chem Supply, #PA054-500 G], 5 mM D-glucose anhydrous [Chem Supply, #GA018-500 G], 2 mM $CaCl_2$ [Scharlau, #CA01951000], and 2 mM $MgCl_2$ [Sigma, #M8266-100 G], pH 7.40) before imaging at room temperature (23°C).[2,29,30] Emissions for Fura-2 were measured at 510 nm, after excitation at 340 and 380 nm, using a Nikon TE300 Eclipse microscope equipped with a Sutter DG-4/OF wavelength switcher, an Omega XF04 filter set for Fura-2, and a Retiga-ELECTRO CCD monochrome cooled camera, operated by MetaFluor software. Retrogradely traced bladder DRG neurons were identified by the presence of the CTB-488, visible with excitation at 480 nm. Fluorescence images at 340 and 380 nm were obtained every 2 seconds using a ×20 objective. Data were recorded and further analysed using MetaFluor software.

After an initial baseline reading to ensure cell fluorescence was stable, indicating healthy cells, DRG neurons were stimulated with 5-HT (100 μM; Merck, #H9523), ATP (10 μM; Merck #1852), and Capsaicin (1 μM; Merck, #M2028), with changes in intracellular calcium ($Ca^{2+}{}_i$) monitored in real time in the presence or absence of TTA-A2 (10 μM; Alomone lab, T-140). Addition of agonists (60 seconds) was performed in sequence on a single coverslip with washout periods (4 minutes) between each compound. $Ca^{2+}{}_i$ is expressed as the ratio between the fluorescence signals at 340 and 380 nm (Fura-2 [340/380]) and normalised to a baseline fluorescence of 1.

2.8. Immunohistochemistry

2.8.1. Staining

Cultured DRG neurons from $Na_v1.8$Cre-TdTomato mice plated onto glass coverslips were washed 3 times for 5 minutes, each in 0.1 M sterile PBS. Phosphate buffered saline was aspirated and the cells were fixed with 2 mL per well PFA 4% and left in the fridge for 20 minutes. The PFA was removed and the cells were washed 3 times for 5 minutes each in 0.1 M PBS with 0.2% Triton-TX 100 (T-PBS) (Sigma-Aldrich). Cells were incubated with 50 μL rabbit Anti-Cav3.2 (1:200, Alomone Labs) or T-PBS (negative control) prepared in saponin + FBS in the fridge overnight in a humidified chamber. The following day, coverslips were washed with T-PBS (3 times × 5 minutes). Fifty microliters of fluorescent-conjugated secondary antibodies (Alexa Fluor 647 goat anti-rabbit, 1:200; Thermofisher) prepared in PBS + FBS 2% was applied to each coverslip and left at room temperature in the dark for 2 hours. Coverslips were again washed with T-PBS (3 times × 5 minutes) before mounting in Prolong Gold Antifade and cover slipped. Slides were allowed to dry for 24 hours before visualization. Antibody has been previously validated in a $CACNA1H^{-/-}$ mice.[63]

2.8.2. Microscopy

Fluorescence was visualised with confocal laser scanning microscope (Leica TCS SP8X; Leica Microsystems, Wetzlar, Germany). Images (1024 × 1024 pixels) were obtained using ×20 oil objectives. Separation of fluorophores was achieved using white line laser tuned to 488 nm excitation and 503 to 538 nm emission detection settings for AF-488 and 561 nm excitation and 570 to 625 nm emission detection settings for Td-Tomato. Confocal settings were optimized to reduce background staining by adjusting the white light laser intensity, emission window, and amplifier gain. These settings were saved and used for all imaging. Images were processed and analysed using Image J

software (NIH). Other than making moderate adjustments for contrast and brightness, the images were not manipulated in any way.

2.9. Visceromotor response to bladder distension

Visceromotor response (VMR) to bladder distension has previously been performed and characterised in both mice and rats.[57,59,66] In this study, guinea pigs were anaesthetised with urethane (1.2 g/kg s.c.) and inhaled isoflurane and placed on a heating pad to maintain body temperature at 37˚C. Depth of anaesthesia was assessed by lack of response to hind limb pinch. Right external jugular vein was dissected of the surrounding tissue to allow administration of drugs. A 3-mm o.d. catheter (2.5 mm i.d.) was pulled to have approximately 0.5-mm tip diameter and inserted into the bladder dome and then tied securely in place with purse-like 5.0 ligatures. The catheter was attached to a T-piece adaptor, the left arm of which was connected to a PBS-containing 20-mL syringe, relative position of which (to guinea pig) can be changed and fixed. The right arm of the T-piece was connected to a pressure transducer (Viggo-Spectramed model P23XL, Oxnard, CA) to measure changes in the intravesical pressure. Electromyographic (EMG) electrodes were placed into the left external oblique muscle and a reference electrode placed in the soleus muscle of the opposing leg. Once EMG electrodes were implanted, there was a 20-minute rest period before distension began. At this time, isoflurane was withdrawn and mice were anaesthetised with only urethane for the VMR distensions, so spinal reflexes could be maintained.[37]

The external urethral meatus was clamped and after 5 to 10 minutes pause, 60 mm Hg (for 20 seconds) bladder distension, evoked by raising a column of water (PBS), was repeated 4 times (with 5-minute interval) until 2 last successive responses were similar. Then, 2 stimulus–response curves were produced by using the following protocol: intravesical pressure was increased by raising a column of water (PBS) in 10 or 20 mm Hg increments, from 0 mm Hg to 10, 20, 40, 50, and 60 mm Hg (for 20 seconds each), with a 5-minute interval between single distension and between each curve. Thirty minutes after administration of TTA-A2 (3 mg/kg, in 100 μL DMSO) into the jugular vein, 2 stimulus–response curves were repeated as described above. DMSO alone had no significant effects on distension response. Intravesical pressures of 10 and 20 mm Hg were chosen to reflect physiological levels of bladder distension, whereas 40, 50, and 60 mm Hg represent noxious levels of bladder distension.

Both intravesical pressure and EMG activity were recorded with a MacLab 8sp (AD Instruments, Castle Hill, NSW, Australia) by using Chart 7 software (AD Instruments). Electromyography recordings were acquired at 10 kHz, high pass filtered (50 Hz), rectified, and integrated. The area under the curve (AUC, in μV) at each distension pressure was corrected for the baseline activity by subtracting a 20-second baseline immediately before each distension, from the 20-second distension. Total AUC was quantified by summing the individual AUC at each distension pressure.

2.10. Experimental design and statistical analyses

Data are presented as mean ± SEM or the % of afferents or neurons. Within the specific figure legends, N indicates the number of animals, while n indicates the number of independent afferents or neurons. Sample size was based on historical data and the use of power calculations. Statistical significance was reported at levels of */^$P < 0.05$, **/^^$P < 0.01$, and ***/$$P < 0.001$. In some cases, because of space limitation, # is used to indicate significance of $P < 0.001$ for multiple comparisons. Data were tested for Gaussian distribution using Prism 8 (GraphPad, San Diego, CA) to determine if they were normally distributed or not and therefore the correct statistical tests to be used. Data were then analysed accordingly using Prism 9 (GraphPad) by 1- or 2-way analysis of variance (ANOVA) with Tukey or Sidak post hoc analyses dependent on data distribution, or Student *t* tests, for parametric data. The specific tests used for analysis of each data set are indicated within the individual figure legends.

3. Results

3.1. $Ca_V3.2$ is expressed in bladder-innervating sensory neurons

To investigate if a specific subtype of Ca_V3 channel is predominant within peripheral bladder sensory pathways, we determined the expression of $Ca_V3.1$, $Ca_V3.2$, and $Ca_V3.3$ channels in bladder-innervating sensory neurons isolated from mice (**Fig. 1A**). Single-cell RT-PCR revealed $Ca_V3.2$ is expressed in 79.5% (70/88 neurons) of bladder-innervating DRG retrogradely traced from the bladder (**Figs. 1Ai, Aii**). In contrast, $Ca_V3.1$ (1/88 neurons) and $Ca_V3.3$ (0/88 neurons) were barely or not expressed in the cell bodies of bladder-innervating sensory neurons (**Figs. 1Ai, Aii**). All cells were confirmed to be neuronal through expression of neuronal marker *tubb3* (**Fig. 1Ai**). In whole LS DRG, $Ca_V3.2$ exhibited significantly higher expression than $Ca_V3.1$ and $Ca_V3.3$, whereas $Ca_V3.1$ was barely above the level of detection (**Fig. 1Bi**). $Ca_V3.2$ also showed significantly higher expression than TRPV1 (**Fig. 1Bi**), a highly expressed target in DRG neurons. High levels of $Ca_V3.1$ and $Ca_V3.3$ were found in the brain (**Fig. 1Bii**). Antibody staining for $Ca_V3.2$ in isolated DRG neurons from $Na_V1.8$-TdTomato mice confirmed $Ca_V3.2$ was expressed in LS DRG neurons innervating the bladder (**Fig. 1C**).

3.2. $Ca_V3.2$ regulates bladder-afferent responses to distension

The relative abundance of $Ca_V3.2$ in whole lumbosacral DRG and the high proportion of bladder-innervating neurons expressing $Ca_V3.2$ suggests that previously observed effects of $Ca_V3.2$ inhibition on bladder function[42,54,60] may be regulated through modulation of bladder sensory neuron excitability.

To explore the role of $Ca_V3.2$ in bladder sensation, we utilised a well-characterised ex vivo bladder afferent preparation allowing simultaneous recording of intravesical pressures and mechanosensitive afferent firing during repeated bladder distensions[8,29,35] (**Fig. 2**). We utilised 2 selective blockers of T-type calcium channels, ABT-639 and TTA-A2. Although both ABT-639 and TTA-A2 inhibit $Ca_V3.1$, $Ca_V3.2$, and $Ca_V3.3$, as we showed there was almost no expression of $Ca_V3.1$ and $Ca_V3.3$ in bladder-innervating DRG neurons (with 79.5% expressing $Ca_V3.2$), ABT-639 and TTA-A2 allowed us to probe a more specific role of $Ca_V3.2$ in bladder afferent function.

After an acclimatisation period, repetitive bladder filling evokes reproducible afferent responses to distension characterised by a graded increase in bladder afferent excitability from 0 to 50 mm Hg (**Figs. 2A–C**). Replacing the saline in the infusion pump with ABT-639 or TTA-A2 attenuated bladder afferent firing during subsequent distensions (**Figs. 2A–C**). Both ABT-639 and TTA-A2 significantly reduced the overall AUC (**Figs. 2Aii, Bii, Cii**) and the peak afferent response to distension (**Figs. 2Aiii, Biii, Cii**).

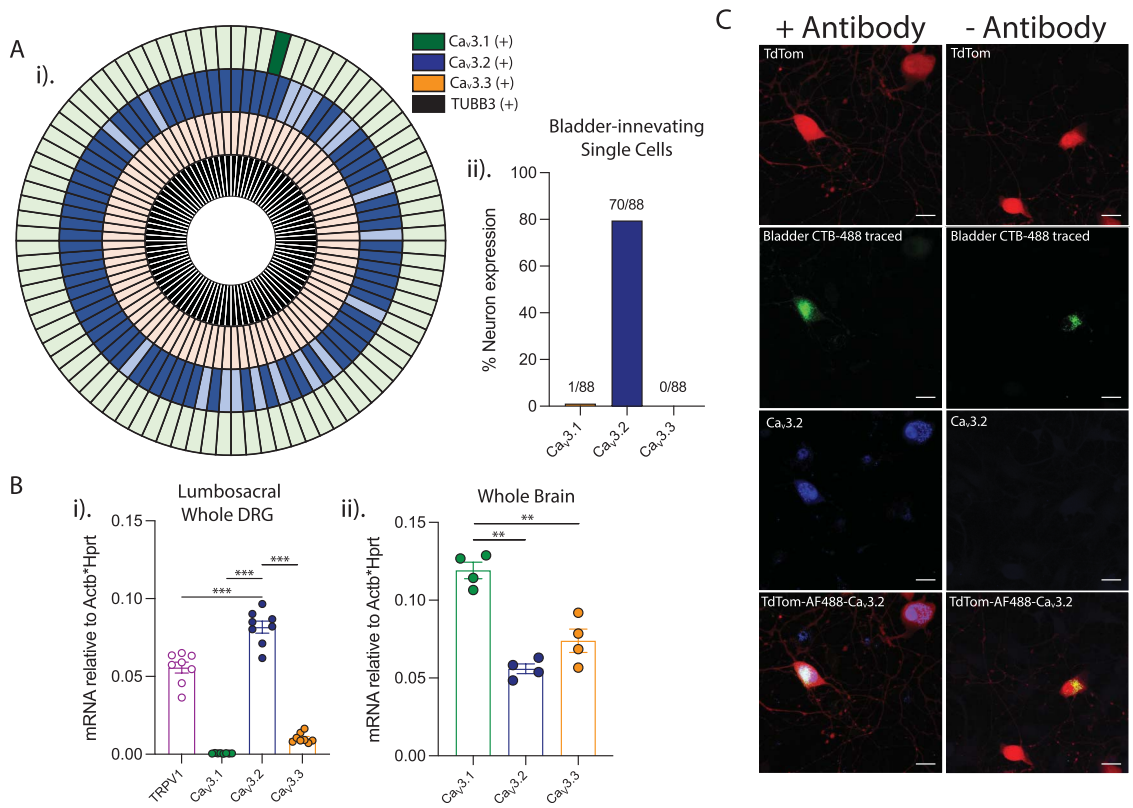

Figure 1. $Ca_V3.2$ is expressed in bladder-innervating sensory neurons. (A) Single-cell RT-PCR of retrogradely traced bladder-innervating DRG neurons reveals the percentage of neurons expressing and co-expressing genes encoding Ca_V3 channels (n = 88 single cells from N = 8 mice). (Ai) Donut plot showing expression and co-expression of genes encoding $Ca_V3.1$, $Ca_V3.2$, and $Ca_V3.3$ in bladder-innervating DRG neurons. Each colour represents an individual gene with expression marked by bold colouring. Individual neurons are arranged radially, such that co-expression of genes in a single neuron can be easily identified running from outside to inside. (Aii) mRNA for $Ca_V3.2$ was expressed in 79.5% (70/88) of bladder-innervating DRG neurons. In contrast, $Ca_V3.1$ and $Ca_V3.3$ were expressed in 1/88 and 0/88 bladder-innervating DRG neurons, respectively. (Bi) QRT-PCR was used to determine mRNA expression of Ca_V3 receptor subtypes $Ca_V3.1$, $Ca_V3.2$, and $Ca_V3.3$ and TRPV1 relative to *Actb and Hprt* in pooled lumbosacral (L5, L6, and S1) dorsal root ganglia (DRG; N = 8). $Ca_V3.2$ was significantly more abundant than $Ca_V3.3$ (***$P < 0.001$), $Ca_V3.1$ (***$P < 0.001$), and TRPV1 (**$P < 0.01$). (Bii) QRT-PCR was used to determine mRNA expression of Ca_V3 receptor subtypes $Ca_V3.1$, $Ca_V3.2$, $Ca_V3.3$ relative to *Actb and Hprt* in whole brain tissue (N = 4). (C) Antibody staining for $Ca_V3.2$ in isolated bladder-innervating lumbosacral DRG. $Ca_V3.2$ is abundantly expressed in the peripheral sensory neurons from $Na_V1.8$Cre-TdTomato mice in primary culture (left panel). $Ca_V3.2$-like immunoreactivity is absent when the primary antibody is omitted (right panel). Scale bars = 20 μm. Data are represented as mean ± SEM (A). *P* values were determined by 1-way ANOVA with subsequent Tukey multiple comparison post hoc test (Bi, Bii). RT-PCR data are represented as percentage of neurons (Aii) or mean ± SEM ($2^{-\Delta Ct}$) on a linear scale (Bi, Bii). ANOVA, analysis of variance; DRG, dorsal root ganglia; QRT-PCR, quantitative reverse-transcription polymerase chain reaction; RT-PCR, reverse-transcription polymerase chain reaction; TdTom, TdTomato.

Changes in bladder afferent firing in response to distension occurred without changes in bladder compliance, which reflects the ability of the bladder muscle to accommodate an equivalent bladder volume (**Figs. 2Aiv, Biv, Cii**). As such, these data suggest that T-type calcium channel $Ca_V3.2$ regulates bladder afferent responses to distension via direct inhibition of bladder-innervating sensory afferent nerves.

3.3. TTA-A2 inhibits the majority of distension sensitive bladder afferents

The pelvic nerve strand that was recorded from in each bladder-nerve recording experiment (**Fig. 2**) contained between 5 and 18 single mechanosensitive afferent units. By matching individual spike waveforms through linear interpolation, it was possible to perform post hoc analysis on these individually identified single afferent units[30] (**Fig. 3**). Analysing our data in this way reduces intraexperimental variability and revealed a significant inhibitory effect of 100 μM ABT-639 and 10 to 100 μM TTA-A2 on bladder afferent responses to distension (**Fig. 3Ai, ii, iii**), with TTA-A2 having a greater overall inhibitory effect than ABT639 (**Fig. 3Aiii**); 90% (80/88, 100 μM TTA-A2) and 65% (26/40, 100 μM ABT-639) of total single units exhibited greater than a 25% reduction in their AUC over the distension period (**Fig. 3Aiii**). Both ABT-639 and TTA-A2 at 100 μM significantly inhibited the overall bladder afferent response to distension, the peak afferent response to distension, and significantly delayed the activation thresholds for bladder distension–evoked afferent firing (**Figs. 3Bi, ii, Ci, ii**). Although 10 μM TTA-A2 had no impact on peak afferent response (**Fig. 3Ci**), it did increase afferent activation thresholds to bladder distension (**Fig. 3Cii**). No gender differences were observed in the ability of 100 μM TTA-A2 to inhibit bladder afferent responses to distension (Supplementary Figure 1, available at http://links.lww.com/PAIN/B743). Single units from male and female mice had peak afferent responses inhibited by 61.3% and 63.7% and total AUC responses inhibited by 66.7% and 63.6%, respectively (Supplementary Figure 1A, B, available at http://links.lww.com/PAIN/B743).

3.4. TTA-A2 inhibits both low- and high-threshold bladder afferents

Based on the activation threshold under control filling conditions, distension-sensitive bladder afferents can be differentiated into

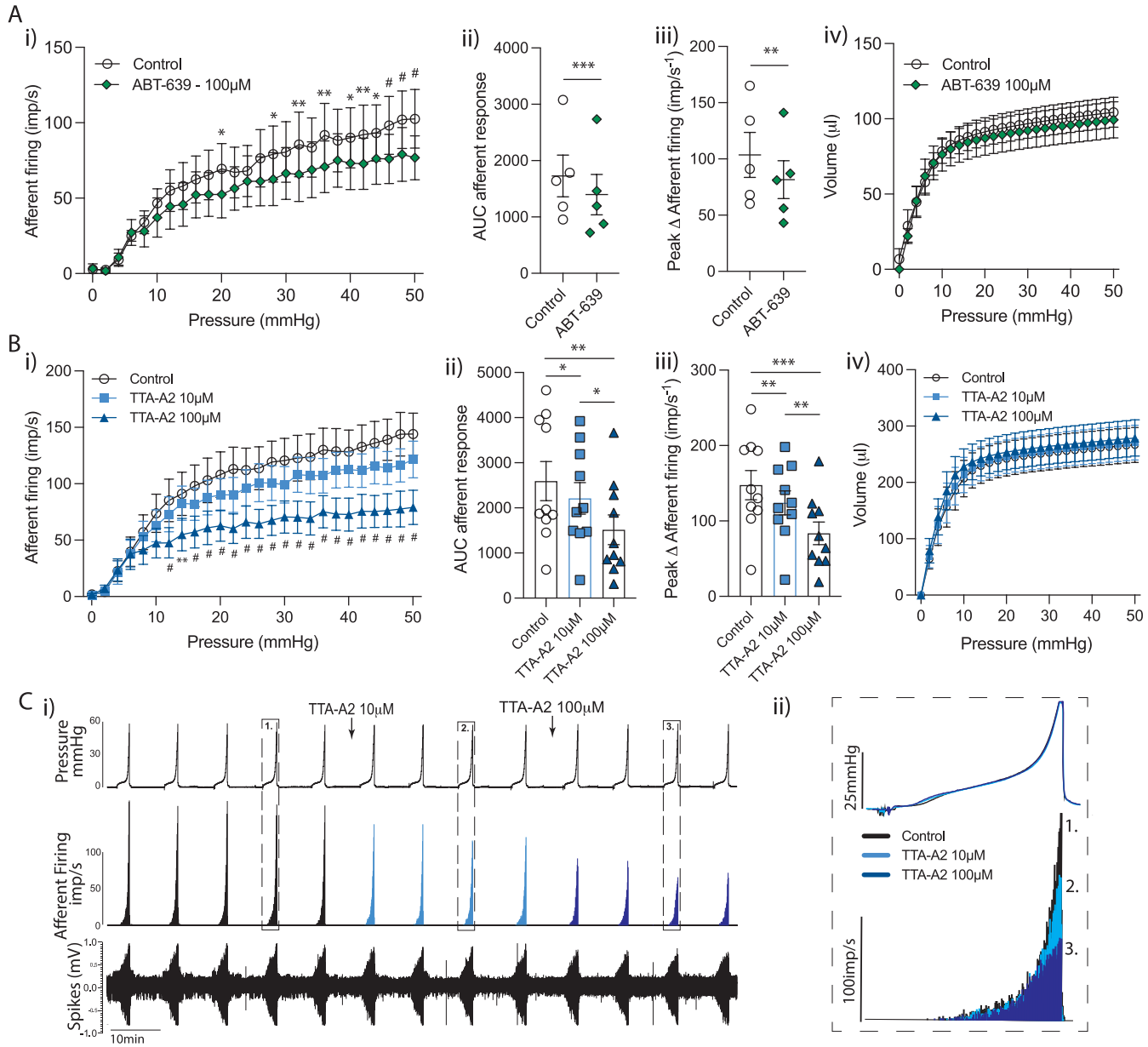

Figure 2. ABT-639 and TTA-A2 inhibit bladder afferent mechanosensitivity to graded bladder distension ex vivo via $Ca_V3.2$. Graded distension of the bladder (0-50 mm Hg) in an ex vivo bladder-nerve recording preparation was performed with saline followed by ABT-639 or TTA-A2. (Ai) Intrabladder instillation of 100 μM ABT-639 (green) resulted in a decrease in afferent firing rate (impulses per second; imp/s) compared with saline (black) at distension pressures at and above 20 mm Hg (N = 5; $^*P < 0.05$; $^{**}P < 0.01$; $\#P < 0.001$). (Aii) ABT-639 decreased the total area under the curve (AUC) of the afferent response to distension (N = 5; $^{***}P < 0.001$) and (Aiii) peak afferent firing rate (N = 5; $^{**}P < 0.01$, Δ = 22 ± 17 imp/s). (Aiv) Bladder muscle compliance (pressure/volume relationship) was unaffected by 100 μM ABT-639. (Bi) Administration of 100 μM TTA-A2 (dark blue) but not 10 μM TTA-A2 (light blue) resulted in a decrease in afferent firing rate to graded bladder distension (0-50 mm Hg) compared with saline (black) at distension pressures at and above 12 mm Hg (N = 10; $^*P < 0.05$; $^{**}P < 0.01$; $\#P < 0.001$). (Bii) TTA-A2 (10 and 100 μM) decreased the total area under the curve (AUC) of the afferent response to distension (N = 10; $^*P < 0.05$, $^{**}P < 0.01$) and (Biii) peak afferent firing rate (N = 10; $^*P < 0.01$, Δ = 24 ± 16 imp/s, $^{***}P < 0.001$, Δ = 64 ± 15 imp/s). (Biv) Bladder muscle compliance (pressure/volume relationship) was unaffected by 10 to 100 μM TTA-A2. (Ci) Experimental trace showing a dose-dependent decrease in raw afferent nerve activity in the presence of 10 to 100 μM TTA-A2 during repetitive bladder distensions (0-50 mm Hg) at 10-minute intervals. (Cii) Overlaid intravesical pressure and afferent response traces from dashed boxes in (Ci) before and during intrabladder instillation with 10 to 100 μM TTA-A2. Bladder afferent, but not pressure, responses to bladder filling were significantly altered. Data are represented as mean ± SEM (A and B). *P* values are based on 2-way ANOVA with subsequent Sidak post hoc test significance at individual data points indicated on (Ai, Aiv, Bi, and Biv), paired *t* test (Aii and Aiii), or 1-way ANOVA with subsequent Tukey post hoc test (Bii and Biii). ANOVA, analysis of variance.

low- and high-threshold subtypes.[35] Both low- and high-threshold bladder afferents were present in all multiunit recordings, and both subtypes were dose-dependently inhibited by TTA-A2 (10-100 μM) and ABT-639 (**Fig. 4Ai–v**). ABT-639 and TTA-A2 had a larger inhibitory effect in high-threshold afferents, with TTA-A2 also causing greater inhibition than ABT-639, which almost abolished high-threshold afferent responses to distension (**Figs. 4Aiv, Av, B**). ABT639 and TTA-A2 significantly inhibited peak afferent responses and delayed the activation threshold of both low- and high-threshold afferents (**Figs. 4Ci–iv, 4Di–iv**). The delay in activation threshold of distension-sensitive afferents with TTA-A2 increased the proportion of afferents with activation thresholds greater than 30 mm Hg, such that they would no longer respond to physiological levels of bladder distension.

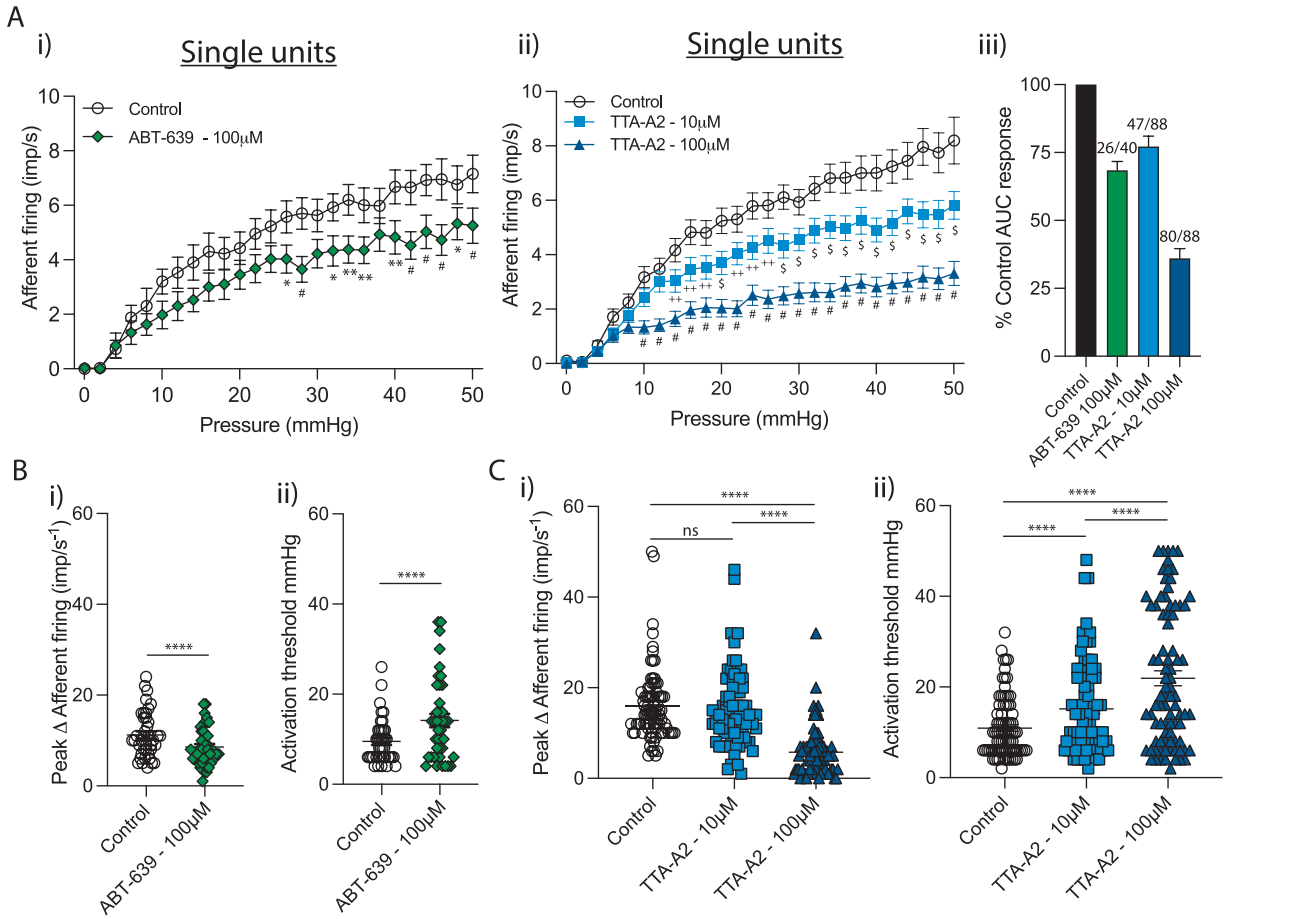

Figure 3. ABT-639 and TTA-A2 inhibit single-unit bladder afferent responses to distension. Post hoc waveform analysis allows for the identification of single mechanosensitive units from multiunit bladder-nerve recordings. One hundred twenty-eight distinct single units were extracted from 15 multiunit experiments. (Ai) 100 μM ABT-639 significantly inhibited bladder afferent firing rate to graded bladder distension (impulses per second; imp/s) compared with saline (black); (control vs 100 μM ABT-639; n = 40; $^{*}P < 0.05$; $^{**}P < 0.01$; $^{\#}P < 0.001$). (Aii) Graded bladder distensions with 10 μM (light blue) and 100 μM (dark blue) TTA-A2 significantly inhibited bladder afferent firing rate to graded bladder distension (impulses per second; imp/s) compared with saline (black); (control vs 10 μM TTA-A2; n = 88; $^{++}P < 0.01$; $^{\$}P < 0.001$); (control vs 100 μM TTA-A2; n = 88; $^{**}P < 0.01$; $^{\#}P < 0.001$). (Aiii) The AUC of the afferent response to distension (0-50 mm Hg) was reduced from control by 32 ± 3.2% (100 μM ABT-639, 26/40 units inhibited), 23 ± 3.9% (10 μM TTA-A2, 47/88 units inhibited), and 64 ± 3.6% (100 μM TTA-A2, 80/88 units inhibited). (Bi) Peak afferent firing rate (imp/s^{-1}) of individual bladder afferent units before (control) and after 100 μM ABT-639 (n = 40; $^{****}P < 0.001$). Sixty-five percent of single units were sensitive to the inhibitory effects of 100 μM ABT-639, exhibiting a greater than 25% reduction in overall excitability. (Bii) Activation thresholds (mm Hg) of individual bladder afferent units before (control) and after 100 μM ABT639 (n = 40; $^{***}P < 0.001$). (Ci) Peak afferent firing rate (imp/s^{-1}) of individual bladder afferent units before (control) and after 10 to 100 μM TTA-A2 (control vs 10 μM TTA-A2, n = 88; ns $P > 0.05$; control vs 100 μM TTA-A2, n = 88; $^{****}P < 0.001$; 10 μM vs 100 μM TTA-A2, n = 88; $^{****}P < 0.0001$). The vast majority (89%) of single units were sensitive to the inhibitory effects of 100 μM TTA-A2, exhibiting a greater than 25% reduction in overall excitability. (Cii) Activation thresholds (mm Hg) of individual bladder afferent units before (control) and after 10 to 100 μM TTA-A2 (control vs 10 μM TTA-A2, n = 88; $^{*}P < 0.05$; control vs 100 μM TTA-A2, n = 88; $^{***}P < 0.001$; 10 μM vs 100 μM TTA-A2, n = 46; $^{***}P < 0.001$). Data are represented as mean ± SEM. *P* values were determined by either 2-way ANOVA with subsequent Sidak multiple comparison post hoc test (Ai, Aii), paired *t* test (Bi, Bii), or 1-way ANOVA with subsequent Tukey multiple comparison post hoc test (Ci, Cii). ANOVA, analysis of variance; AUC, area under the curve.

3.5. TTA-A2 inhibits the visceromotor response to bladder distension in vivo

To determine if inhibiting T-type calcium channels was also able to reduce bladder sensory signalling in vivo, we investigated the effect of TTA-A2 on the VMRs to bladder distension (**Fig. 5**). The VMR, assessed by recording the electrical activity (EMG) produced by abdominal muscle contractions, is often characterised as a nocifensive response to acute visceral stimuli. A VMR in response to noxious (>40 mm Hg) bladder distension has thus been established as a surrogate marker for bladder pain.[56,58,66] In anaesthetised guinea pigs, i.v. administration of TTA-A2 was able to significantly reduce VMRs to increasing bladder distension pressures (**Figs. 5A–C**). Total area under the curve (AUC) of the EMG response to all distension pressures (10, 20, 40, 50, and 60 mm Hg) was significantly reduced after TTA-A2 administration (**Fig. 5C**).

3.6. Intracellular calcium (iCa^{2+}) responses to 5-HT, ATP, and capsaicin in bladder-innervating dorsal root ganglia neurons were unaffected by TTA-A2

Using single-cell RT-PCR of isolated bladder-innervating DRG, we discovered high levels of colocalization between $Ca_V3.2$ and receptors/ion channels that have been shown to regulate bladder afferent signalling, including TRPV1 (93%), $P2X_3$ (85%), and $5HT_{3A}$ (93%) (**Figs. 6A and B**).[15,17,33,49,77,81] Live-cell calcium imaging of bladder-innervating DRG was used to determine if $Ca_V3.2$ inhibition with TTA-A2 also regulated neuronal activation induced by TRPV1, P2X, and 5-HT_3 agonists (**Figs. 6C–F**). Retrogradely traced bladder-innervating DRG neurons were identified via AF-488 fluorescence (**Fig. 6Ci**), and neuronal activation was measured by an increase in intracellular calcium (iCa^{2+}) determined with Fura-2 as a ratio of emissions after excitation at 340 and 380 nm light (**Figs. 6Cii, Ciii, Civ**). Bladder

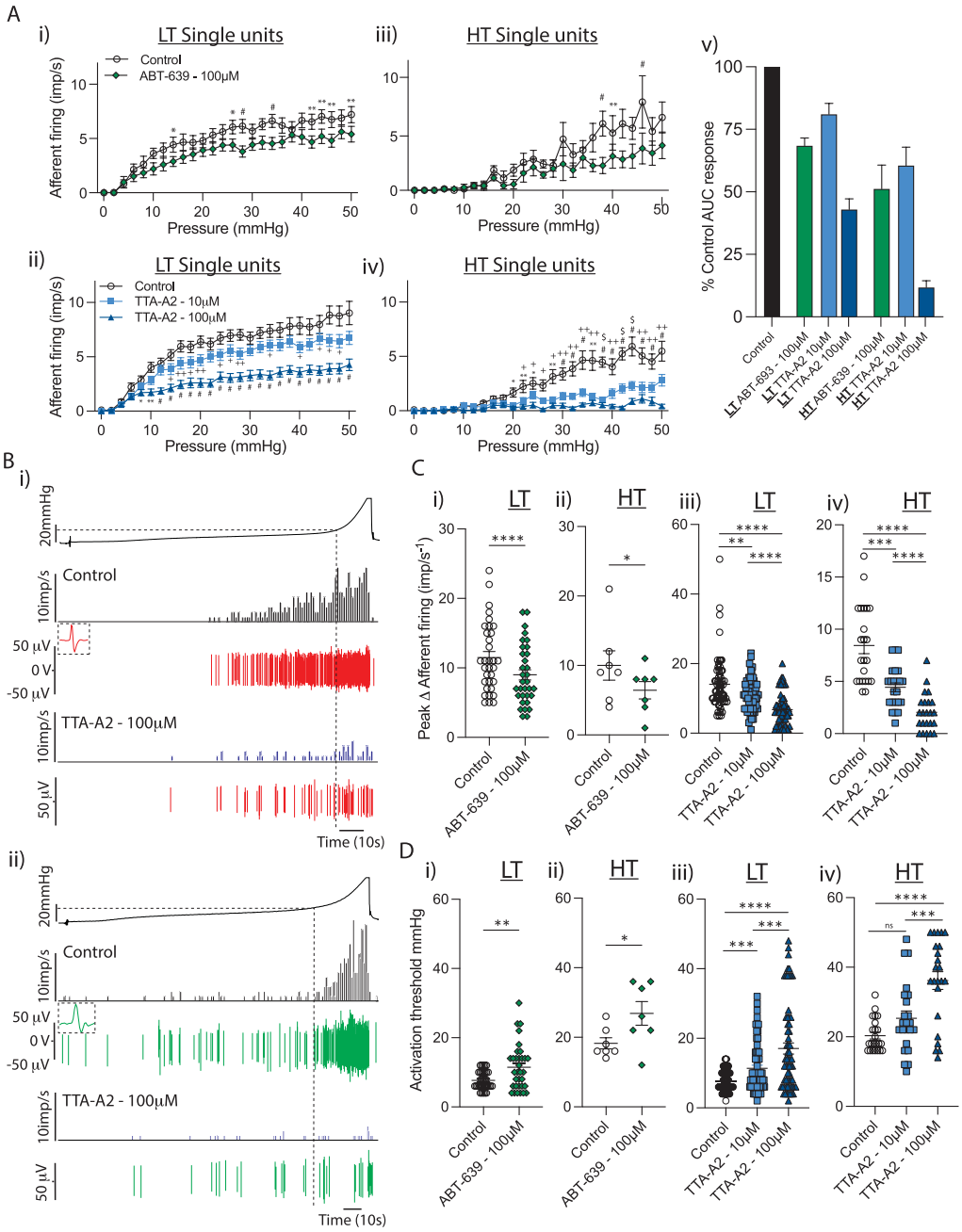

Figure 4. ABT-639 and TTA-A2 inhibit low- and high-threshold mechanosensitive bladder afferents. Bladder afferents can be distinguished based on their activation threshold to distension as either low or high threshold. (Ai) ABT-639 and (Aii) TTA-A2 significantly attenuated low-threshold afferent mechanosensitivity (control vs 100 μM ABT-639, n = 33; $^{*}P < 0.05$; $^{**}P < 0.01$; $^{\#}P < 0.001$); (control vs 10 μM TTA-A2, n = 65; $^{+}P < 0.05$; $^{++}P < 0.01$; $^{\$}P < 0.001$); (control vs 100 μM TTA-A2, n = 65; $^{**}P < 0.01$; $^{\#}P < 0.001$). (Aiii) ABT-639 and (Aiv) TTA-A2 also significantly attenuated high-threshold afferent mechanosensitivity (control vs 100 μM ABT-639, n = 7; $^{**}P < 0.01$; $^{\#}P < 0.001$); (control vs 10 μM TTA-A2, n = 23; $^{+}P < 0.05$; $^{++}P < 0.01$; $^{\$}P < 0.001$); (control vs 100 μM TTA-A2, n = 16; $^{*}P < 0.05$; $^{**}P < 0.01$; $^{\#}P < 0.001$). (Av) ABT-639 and TTA-A2 (10-100 μM) had a larger inhibitory effect in high threshold (HT) afferents, and inhibited a great proportion of high-threshold than low-threshold afferents (10 μM TTA-A2 14/23 vs 32/65, 100 μM TTA-A2 23/23 vs 57/65, 100 μM ABT-693 6/7 vs 20/33). (B) Example experimental traces showing mechanosensitivity of a single low-threshold afferent unit (Bi) and a single high-threshold afferent unit (Bii) in response to graded bladder distensions (0-50 mm Hg) before (control) and after 100 μM TTA-A2. Individual units are identified by spike waveform profiling (inserts) and represented by different colour spike profile. Dashed line represents the cut-off for low/high activation threshold (C) Peak afferent response of low- and high-threshold bladder afferents to distension in the presence of ABT-639 (Ci and Cii) and TTA-A2 (Ciii and Civ). ABT-639 significantly reduces peak afferent firing in low threshold (LT) (Ci) (n = 33; $^{****}P < 0.0001$) and HT (Cii) (n = 7, $^{*}P < 0.05$) bladder afferents. TTA-A2 significantly reduces peak afferent firing in low threshold (Ciii) (control vs 0.10 μM TTA-A2, n = 65; $^{**}P < 0.01$; control vs 100 μM TTA-A2, n = 65; $^{****}P < 0.0001$; 10 μM vs 100 μM TTA-A2, n = 65; $^{****}P < 0.0001$); and high threshold bladder afferents (Civ) (control vs 10 μM TTA-A2, n = 23; $^{*}P < 0.05$; control vs 100 μM TTA-A2, n = 23; $^{****}P < 0.0001$; 10 μM vs 100 μM TTA-A2, n = 23; $^{****}P < 0.0001$). (D) Activation threshold (mm Hg) of low- and high-threshold bladder afferents to distension in the presence of ABT-639 (Di, Dii) and TTA-A2 (Diii, Div). ABT-639 significantly increased activation thresholds of LT (Di) (n = 33; $^{****}P < 0.01$); and HT (Dii) (n = 7, $^{*}P < 0.05$) bladder afferents. TTA-A2 significantly increased the activation thresholds of low threshold (Ciii) (control vs 10 μM TTA-A2, n = 65; $^{***}P < 0.001$; control vs 100 μM TTA-A2, n = 65; $^{****}P < 0.0001$; 10 μM vs 100 μM TTA-A2, n = 65; $^{****}P < 0.0001$) and high threshold afferents to distension (Div) (control vs 10 μM TTA-A2, n = 23; ns $P > 0.05$; control vs 100 μM TTA-A2, n = 23; $^{****}P < 0.01$; 10 μM vs 100 μM TTA-A2, n = 23; $^{***}P < 0.001$). *P* values were determined by either 2-way ANOVA with subsequent Sidak multiple comparison post hoc test (Ai-iv), paired *t* test (Ci, Cii, Di, and Dii) or 1-way ANOVA with subsequent Tukey multiple comparison post hoc test (Ciii, Civ, Diii, and Div).

traced neurons exhibited robust iCa^{2+} responses to sequential administration of 5-HT, ATP, and capsaicin (**Fig. 6D**) that were unaffected by prior incubation with TTA-A2 (**Figs. 6E–G**). Overall iCa^{2+} responses were not significantly different between control cells and cells incubated with TTA-A2 (**Fig. 6Ei, Eii, Eiii**). The percentage of bladder-innervating neurons responding to each agonist (**Fig. 6F**), and the peak response to each agonist (**Fig. 6G**), was unchanged in the presence of TTA-A2.

4. Discussion

Normal bladder function relies on the accurate determination of bladder volume via the propagation of sensory signals into the spinal cord and higher brain centres. The intensity of these peripheral sensory signals controls urine storage and micturition and initiates the sensations that inform our conscious control of voiding.[1,4] As such, an increase in the intensity of these sensory signals is thought to underlie the development of common, chronic bladder hypersensitivity disorders including OAB and IC/BPS.[28] Although OAB affects approximately 10% of both men and women, IC/BPS disproportionately affects women, with a female-to-male ratio of around 5:1.[18,36,41,43,70,72]

Transduction of bladder stretch into sensation relies on the detection of mechanical distortion by mechanosensitive ion channels in urothelial cells and bladder afferent nerve terminals,[4,82,83] and the subsequent amplification of this signal to depolarise bladder-innervating afferent nerves. Mounting evidence implies a key role for $Ca_V3.2$ in the regulation/amplification of mechanosensory signals to modulate peripheral sensory signals that are relayed to the CNS.[24,38,48,78,84] The results of our study provide the first evidence to support a major role for $Ca_V3.2$ in regulating bladder afferent firing during filling.

$Ca_V3.2$ inhibition has previously been shown to increase bladder capacity and reduce voiding frequency in a model of bladder overactivity.[42] However, the mechanisms underlying these effects have remained undetermined because of the abundant expression of $Ca_V3.2$ within nonneuronal cells[71,80] and both central and peripheral neuronal structures.[84] Our data support a role for $Ca_V3.2$ in regulating bladder sensation and function via modulation of the excitability of mechanosensitive peripheral afferent nerves. By utilising an ex vivo afferent recording preparation and intravesical infusion of TTA-A2 and ABT-639, we were able to exclude CNS interactions. Additionally, attenuated responses of bladder afferents during bladder distension were observed in the absence of changes to bladder muscle compliance. This is an essential distinction, as even small changes in bladder muscle function can have dramatic impacts on bladder afferent output,[32,39] and confirms that alterations in the contractile force of the bladder wall were not responsible for the changes in afferent excitability we observed. T-type calcium currents have previously been detected in bladder smooth muscle cells[71] where they modulate spontaneous excitation in vitro.[80] However, in line with our data showing no effect of TTA-A2 on detrusor muscle function ex vivo, inhibition of T-type currents does not affect detrusor tone or contractions in vitro or nonvoiding contractions during in vivo cystometry.[42] As such, a functional role of $Ca_V3.2$ in bladder smooth muscle has yet to be determined. Additional evidence that $Ca_V3.2$ contributes to peripheral afferent excitability was found with the significant expression of $Ca_V3.2$ in peripheral bladder sensory pathways. In line with previous reports, we observed predominant expression of $Ca_V3.2$ in lumbosacral DRG over $Ca_V3.1$ and $Ca_V3.3$.[11,61] More importantly, the vast majority of retrogradely traced bladder-innervating sensory neurons expressed $Ca_V3.2$, whereas $Ca_V3.1$ and $Ca_V3.3$ transcripts were almost entirely absent. $Ca_V3.2$ was also observed in the soma of freshly cultured bladder-innervating DRG, suggesting expression of $Ca_V3.2$ is likely to occur in the peripheral terminals of sensory nerves innervating the bladder.

Single-unit analysis of our bladder-nerve recordings revealed that 91% and 65% of distension-sensitive bladder afferents were significantly inhibited by 100 μM TTA-A2 and ABT-639, respectively. Although the concentrations of TTA-A2 and ABT-639 used in this study are relatively high, these compounds are reported to be specific for Ca_V3 channels and are in line with the concentrations previously used to investigate Ca_V3 channel function in vitro and in vivo.[23,40,45,62,74,79] It remains possible that the effects we observed with TTA-A2 and ABT-639 may be a consequence of direct interference with mechanically activated currents in bladder afferent neurons. However, in the absence of genuinely selective inhibitors for the majority of the *bone fide* mechanotransduction ion channels, investigating this limitation was beyond the scope of the current study. For the present study, we must also consider that experimental compounds infused into the bladder are required to overcome the highly impermeable urothelial barrier to target the underlying afferent nerves. We, and

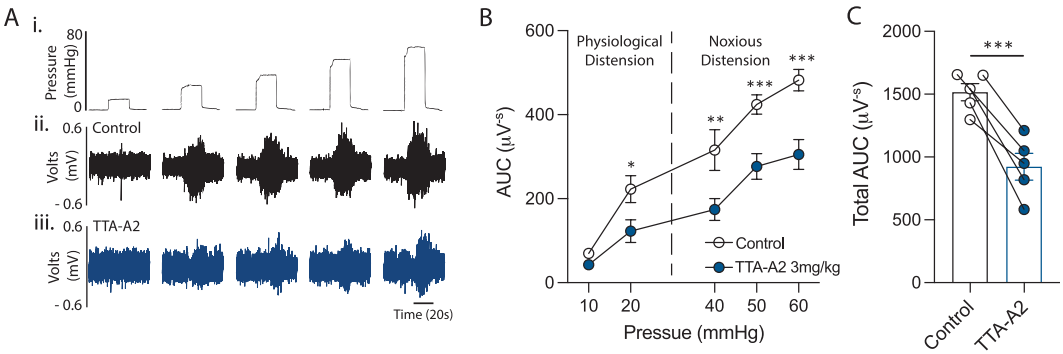

Figure 5. TTA-A2 inhibits the visceromotor response (VMR) to in vivo bladder distension. The VMR to bladder distension in vivo was performed in guinea pigs before and after intravenous (i.v.) injection of 3 mg/kg TTA-A2. (A) Example trace showing electromyography (EMG) response (μV) to bladder distension before (black trace) (Aii) and after IV injection of 3 mg/kg TTA-A2 (dark blue trace). The EMG response to bladder distension is inhibited by TTA-A2. (B) Guinea pigs show an increase in VMR, a nocifensive EMG response of the abdominal muscles, as intravesical distension pressure increases from 10 to 60 mm Hg. TTA-A2 significantly inhibits VMR at distension pressure 20 to 60 mm Hg (N = 5, $^*P < 0.05$, $^{**}P < 0.01$, $^{***}P < 0.001$). (C) Total area under the curve of the EMG response to bladder distension (10-60 mm Hg) was significantly attenuated in all guinea pigs (control vs 3 mg/kg TTA-A2; N = 5, $^{***}P < 0.001$). *P* values are based on either 2-way ANOVA with subsequent Sidak multiple comparison post hoc test (A) or paired *t* test (B). AUC, area under the curve.

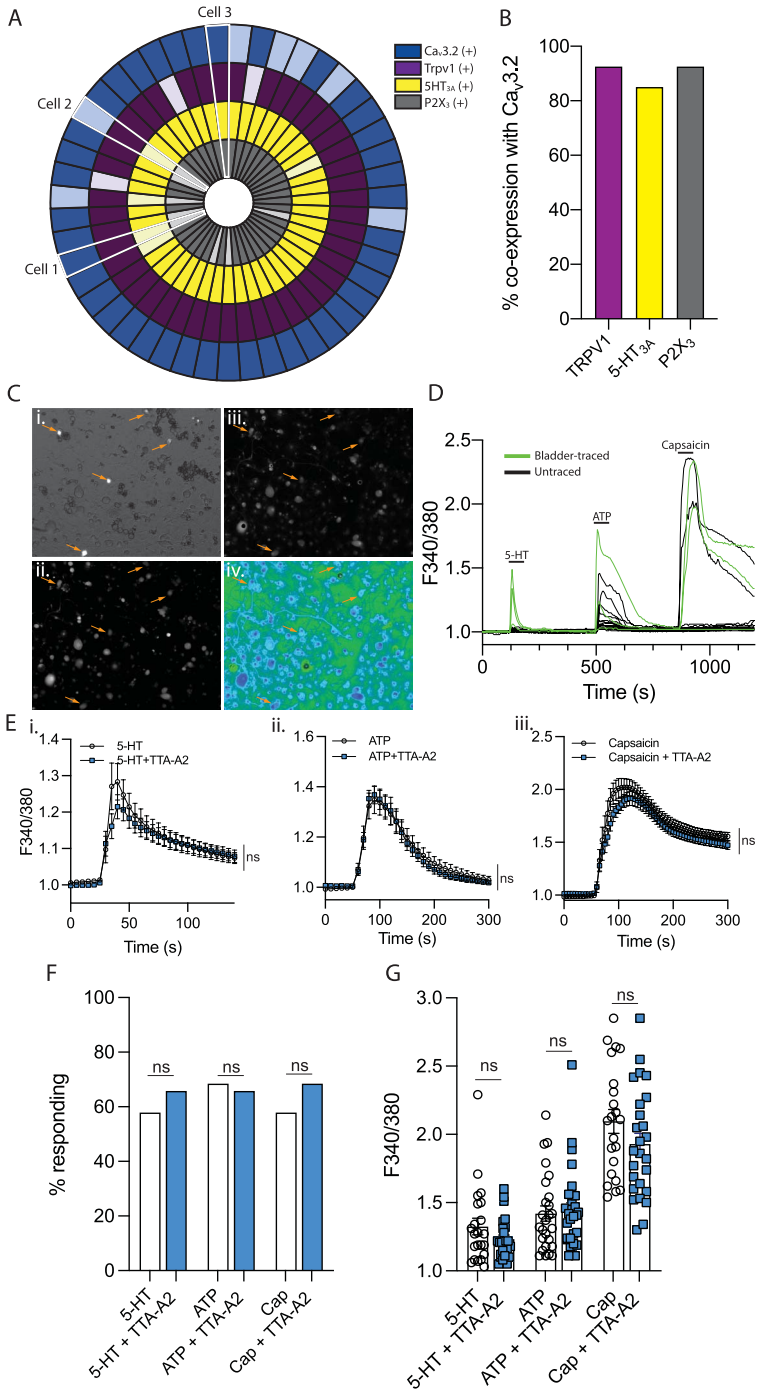

Figure 6. TTA-A2 has no effect on exogenous agonist activation of bladder-innervating DRG neurons. Single-cell RT-PCR of retrogradely traced bladder-innervating DRG neurons revealed the percentage of neurons co-expressing genes encoding $Ca_V3.2$, TRPV1, $P2X_3$, and $5HT_{3A}$. (A) Donut plot showing expression and co-expression of genes encoding $Ca_V3.2$, TRPV1, $P2X_3$, and $5HT_{3A}$ in 47 individual bladder-innervating DRG neurons. Each colour represents an individual gene with expression marked by bold colouring. Individual neurons are arranged radially, whilst cells 1, 2, and 3 highlight the diversity in co-expression of genes in individual neurons. (B) Co-expression of mRNA for $Ca_V3.2$ and all targets were high in bladder-innervating DRG neurons ($Ca_V3.2$ and TRPV1: 93%; $Ca_V3.2$ and $5HT_{3A}$: 85%; $Ca_V3.2$ and $P2X_3$: 93%). (C) Live cell calcium imaging of lumbosacral DRG. (Ci) Retrogradely traced bladder-innervating LS DRG neurons are identified under a fluorescent microscope (with 488 nm excitation and 503-538 nm emission detection). Orange arrows indicate traced neurons. Neurons were excited at 340 and 380 nm light (Cii-iii) to provide an emissions ratio (340/380 nm) (Civ). Low fluorescent ratio (F340/380) during continuous perfusion with control external solution indicates neurons are healthy before the start of experiment (Civ). Bladder-innervating neurons were activated by agonists 5-HT (100 μM), ATP (10 μM), and capsaicin (Cap, 1 μM) as evidenced by an increase in fluorescent ratio (340/380), indicating an increase in intracellular calcium (iCa^{2+}) after channel opening (D–G). (D) Example trace showing increases in iCa^{2+} after sequential administration and washout of 5-HT, ATP, and capsaicin. iCa^{2+} responses to 5-HT (Ei), ATP (Eii), and capsaicin (Eiii) were unchanged in the presence of 10 μM TTA-A2. The percentage of bladder-innervating neurons responding to 5-HT (22/38), ATP (25/38), or capsaicin (22/38) was unchanged by 10 μM TTA-A2—5-HT (25/38), ATP (28/38), capsaicin (26/38) (F). The peak iCa^{2+} responses to 5-HT, ATP, and capsaicin were not significantly altered by 10 μM TTA-A2 (ns $P > 0.05$). P values are based on either 2-way ANOVA with subsequent Sidak multiple comparison post hoc test (E) or 1-way ANOVA with subsequent Tukey multiple comparison post hoc test (F and G). ANOVA, analysis of variance; DRG, dorsal root ganglia; HT, high threshold; LS, lumbosacral; RT-PCR, reverse-transcription polymerase chain reaction.

others, have previously shown that by using higher concentrations of experimental compound, we can overcome this considerable barrier.[29,34,65] Although this does not address the limitation that the exact concentrations at the bladder afferent terminals remain unknown, it is highly likely to be significantly lower than the infused concentration. A more specific role for TTA-A2 and ABT-639 on $Ca_V3.2$ inhibition is supported by our single-cell RT-PCR data identifying 79.5% of bladder-innervating DRG cell bodies expressed mRNA for $Ca_V3.2$. This was nevertheless surprising, as previous research has suggested expression and functional roles for $Ca_V3.2$ is limited to specific subsets of somatic sensory neurons.[24,38] Numerous studies have identified and emphasised a role for $Ca_V3.2$ in regulating peripheral sensation via actions on low-threshold mechanoreceptors innervating D-hair follicles (Aδ-LTMR), an ultrasensitive subpopulation of mechanoreceptors, but not other cutaneous mechanoreceptors nor C-fibre nociceptors.[3,24,68,78] $Ca_V3.2$ was recently shown to be more widely expressed, yet still reasonably restricted, as a selective marker of both C-LTMR and Aδ-LTMR in the skin.[24] The dramatic difference in proportional expression between somatic and bladder-innervating sensory nerves may be a reflection of the significant differences in the anatomy and function of somatic and visceral sensory afferents. Bladder afferents, like in other internal organs, terminate in the organ wall almost exclusively as free nerve endings.[21,25,69] Although different branching patterns have been identified and characterised,[21,69] these morphological structures are comparatively modest compared with the complex sensory structures that innervate the skin. This relative simplicity likely reflects the dramatically narrower sensory remit and function of the bladder compared with the skin, where intricate coding of a variety of distinct stimuli is critical to survival.

Our data do not imply a direct role for $Ca_V3.2$ in mechanotransduction, and this was not the aim of this current study. Previous studies have shown that the low activation threshold of T-type calcium channels places them in a key position for regulating the threshold for action potential generation in neurons.[84] It is likely, therefore, that $Ca_V3.2$ contributes to bladder afferent neuroexcitability, and blocking $Ca_V3.2$ reduces neuronal excitability, thereby decreasing the numbers of action potentials generated in response to mechanical stimuli, in this case bladder distension. Using post hoc single-unit analysis, we showed $Ca_V3.2$ inhibition with TTA-A2 and ABT-639 affected both low- and high-threshold bladder afferents to distension, reducing peak afferent responses and delaying activation thresholds to graded bladder distension. Pharmacological inhibition of T-type channels similarly elevates the mechanical threshold of C-LTMR afferents in a skin-nerve preparation.[24] The threshold for electrically evoked action potential firing in $Ca_V3.2$ expressing cultured DRG is likewise increased with TTA-A2.[23] This increase in the activation threshold of bladder afferents, combined with a reduction in overall firing frequencies, has the potential to exert significant effects on bladder sensation and function by limiting the intensity of the peripheral sensory signals that integrates into CNS circuits.

Bladder afferent pathways project into regions of the spinal cord dorsal horn that activate spinal reflex and projection networks important for regulating storage, micturition, and sensation from the bladder.[5,35] As such, inhibition of peripheral sensory afferents through $Ca_V3.2$ block would be expected to reduce input to these spinal circuits, and ultimately attenuate bladder sensations, particularly those in the noxious range that would signal bladder pain. In support of this concept, we observed significantly attenuated VMR responses to noxious bladder distension in vivo. Targeting T-type Ca_V channels for pain is a well-established concept and has been proposed as a pharmacological target for the treatment of various chronic neuropathic and inflammatory pain conditions.[9] Previous studies have shown that acute cyclophosphamide-induced bladder inflammation in mice evokes an upregulation of $Ca_V3.2$ in the DRG, where it plays an important role in establishing referred hyperalgesia.[40,54] We have recently shown that cyclophosphamide-induced bladder inflammation induces hypersensitivity of predominantly low-threshold wide-dynamic-range mechanosensitive bladder afferents to distension.[55] Together this suggests that the referred hyperalgesia of the pelvic regions observed in this model is because of hyperexcitability of bladder afferent pathways for which $Ca_V3.2$ may play a significant role.

Despite the considerable effects of TTA-A2 on bladder mechanosensitivity, in vitro intracellular calcium (iCa^{2+}) responses of bladder-innervating DRG neurons to 5-HT, ATP, and capsaicin were unchanged by prior incubation with TTA-A2. P2X, 5-HT3, and TRPV1 are nonselective ligand-gated cation channels, which evoke large inward currents when activated to cause membrane depolarisation and action potential firing in excitable cells. The potential contribution of T-type calcium channels in this type of experiment is likely masked by this large ion flux and immediate downstream activation of high-voltage-activated calcium channels and voltage-gated sodium channels. As such, our data indicate that T-type calcium channels do not inhibit excitability of bladder neurons to such an extent that it ubiquitously inhibits their activation by exogenous ligands. However, we cannot rule out a potential role for $Ca_V3.2$ in regulating responses to endogenous agonists at more physiological concentrations. This may have particular relevance to endogenous agonists that regulate bladder afferent responses to distension, such as the irritant sensing Mrgprs, the bile acid receptor TGR5, and histamine 1 receptor, which have recently been shown to induce hypersensitivity of bladder afferents to distension.[10,29,30] The high percentage of bladder-innervating DRG expressing $Ca_V3.2$ increases the likelihood of co-expression of these and other irritant sensing mechanisms within bladder sensory pathways; however, future research will be required to unravel any potential functional interactions. In the present study, the role of $Ca_V3.2$ seems to be more specific, contributing to a regulation of bladder afferent responses to mechanical stimuli. The low-voltage-activated properties of T-type calcium channels that are important for responding to small membrane depolarisations may be a key property that endows suitability for this purpose. Interestingly, the DRG neuron subtype with the highest expression of $Ca_V3.2$ also had highly enriched levels of Piezo2[85]—a key mechanosensory ion channel in the bladder.[53] More recently, $Ca_V3.2$ has also been shown to be an essential mediator of enterochromaffin cell mechanotransduction,[48] and thus, $Ca_V3.2$ may represent a ubiquitous amplifier of mechanosensory signals in peripheral sensory mechanisms. The significant proportion of bladder-innervating DRG expressing $Ca_V3.2$ implies that co-expression with Piezo and other mechanosensitive channels is highly likely within bladder sensory pathways. However, evidence to support genuine functional interactions between mechanosensory channels and $Ca_V3.2$ in the bladder or other mechanosensory organs will require further research.

Bladder hypersensitivity disorders, including OAB and IC/BPS, cause chronic and debilitating illness that severely reduces quality of life for both men and women.[41,70,72] Unravelling the complex neurobiology that regulates bladder afferent mechanosensitivity will be key to the development of effective treatments for bladder hypersensitivity in OAB and IC/BPS.[28] Our data suggests that

$Ca_V3.2$ inhibition is an attractive therapeutic approach for relieving bladder hypersensitivity. Determining the contribution of $Ca_V3.2$ to neuronal hypersensitivity in chronic bladder hypersensitivity conditions warrants further investigation.

Conflict of interest statement

The authors have no conflicts of interest to declare.

Acknowledgements

Work was supported by a National Health and Medical Research Council of Australia (NHMRC) Project Grant (APP1140297 to S. M. Brierley), an NHMRC Investigator Leadership Grant (APP2008727 to S. M. Brierley), an NIH Grant (U01 NS113871 to S. M. Brierley), an Australian Research Council (ARC) Discovery Project (DP220101269 to A. M. Harrington, L. Grundy and S. M. Brierley) and an NHMRC Ideas Grant (APP1184546 to V. Zagorodnyuk).

Appendix A. Supplemental digital content

Supplemental digital content associated with this article can be found online at http://links.lww.com/PAIN/B743.

Article history:
Received 6 December 2021
Received in revised form 31 August 2022
Accepted 9 September 2022
Available online 21 October 2022

References

[1] Árnadóttir J, Chalfie M. Eukaryotic mechanosensitive channels. Annu Rev Biophys 2010;39:111–37.
[2] Bellono NW, Bayrer JR, Leitch DB, Castro J, Zhang C, O'Donnell TA, Brierley SM, Ingraham HA, Julius D. Enterochromaffin cells are gut chemosensors that couple to sensory neural pathways. Cell 2017;170: 185–98.e16.
[3] Bernal Sierra YA, Haseleu J, Kozlenkov A, Bégay V, Lewin GR. Genetic tracing of Ca(v)3.2 T-type calcium channel expression in the peripheral nervous System. Front Mol Neurosci 2017;10:70.
[4] Birder L, Andersson K-E. Urothelial signaling. Physiol Rev 2013;93: 653–80.
[5] Birder LA, de Groat WC. Induction of c-fos expression in spinal neurons by nociceptive and nonnociceptive stimulation of LUT. Am J Physiol 1993; 265:R326–33.
[6] Bourinet E, Alloui A, Monteil A, Barrère C, Couette B, Poirot O, Pages A, McRory J, Snutch TP, Eschalier A, Nargeot J. Silencing of the $Ca_V3.2$ T-type calcium channel gene in sensory neurons demonstrates its major role in nociception. EMBO J 2005;24:315–24.
[7] Bourinet E, Altier C, Hildebrand ME, Trang T, Salter MW, Zamponi GW. Calcium-permeable ion channels in pain signaling. Physiol Rev 2014;94: 81–140.
[8] Brierley SM, Goh KGK, Sullivan MJ, Moore KH, Ulett GC, Grundy L. Innate immune response to bacterial urinary tract infection sensitises high-threshold bladder afferents and recruits silent nociceptors. PAIN 2020; 161:202–10.
[9] Cai S, Gomez K, Moutal A, Khanna R. Targeting T-type/$Ca_V3.2$ channels for chronic pain. Transl Res 2021;234:20–30.
[10] Caldwell A, Grundy L, Harrington AM, Garcia-Caraballo S, Castro J, Bunnett NW, Brierley SM. TGR5 agonists induce peripheral and central hypersensitivity to bladder distension. Sci Rep 2022;12:9920.
[11] Cardoso FC, Castro J, Grundy L, Schober G, Garcia-Caraballo S, Zhao T, Herzig V, King GF, Brierley SM, Lewis RJ. A spider-venom peptide with multitarget activity on sodium and calcium channels alleviates chronic visceral pain in a model of irritable bowel syndrome. PAIN 2021;162:569–81.
[12] Castro J, Harrington AM, Lieu T, Garcia-Caraballo S, Maddern J, Schober G, O'Donnell T, Grundy L, Lumsden AL, Miller P, Ghetti A, Steinhoff MS, Poole DP, Dong X, Chang L, Bunnett NW, Brierley SM. Activation of pruritogenic TGR5, MrgprA3, and MrgprC11 on colon-innervating afferents induces visceral hypersensitivity. JCI Insight 2019;4: 131712.
[13] Choe W, Messinger RB, Leach E, Eckle VS, Obradovic A, Salajegheh R, Jevtovic-Todorovic V, Todorovic SM. TTA-P2 is a potent and selective blocker of T-type calcium channels in rat sensory neurons and a novel antinociceptive agent. Mol Pharmacol 2011;80:900–10.
[14] Choi S, Na HS, Kim J, Lee J, Lee S, Kim D, Park J, Chen CC, Campbell KP, Shin HS. Attenuated pain responses in mice lacking Ca(V)3.2 T-type channels. Genes Brain Behav 2007;6:425–31.
[15] Cockayne DA, Hamilton SG, Zhu Q-M, Dunn PM, Zhong Y, Novakovic S, Malmberg AB, Cain G, Berson A, Kassotakis L, Hedley L, Lachnit WG, Burnstock G, McMahon SB, Ford APDW. Urinary bladder hyporeflexia and reduced pain-related behaviour in P2X3-deficient mice. Nature 2000; 407:1011–15.
[16] Coste B, Crest M, Delmas P. Pharmacological dissection and distribution of NaN/Nav1.9, T-type $Ca2^+$ currents, and mechanically activated cation currents in different populations of DRG neurons. J Gen Physiol 2007; 129:57–77.
[17] Daly D, Rong W, Chess-Williams R, Chapple C, Grundy D. Bladder afferent sensitivity in wild-type and TRPV1 knockout mice. J Physiol 2007; 583:663–74.
[18] Davis NF, Gnanappiragasam S, Thornhill JA. Interstitial cystitis/painful bladder syndrome: the influence of modern diagnostic criteria on epidemiology and on Internet search activity by the public. Transl Androl Urol 2015;4:506–11.
[19] de Groat WC, Griffiths D, Yoshimura N. Neural control of the lower urinary tract. Compr Physiol 2015;5:327–96.
[20] de Groat WC, Yoshimura N. Afferent nerve regulation of bladder function in Health and disease. In: Canning BJ, Spina D, editors. Sensory nerves. Berlin, Heidelberg: Springer Berlin Heidelberg, 2009. p. 91–138.
[21] Forrest SL, Osborne PB, Keast JR. Characterization of axons expressing the artemin receptor in the female rat urinary bladder: a comparison with other major neuronal populations. J Comp Neurol 2014;522:3900–27.
[22] Fowler CJ, Griffiths D, de Groat WC. The neural control of micturition. Nat Rev Neurosci 2008;9:453–66.
[23] Francois A, Kerckhove N, Meleine M, Alloui A, Barrere C, Gelot A, Uebele VN, Renger JJ, Eschalier A, Ardid D, Bourinet E. State-dependent properties of a new T-type calcium channel blocker enhance Ca(V)3.2 selectivity and support analgesic effects. PAIN 2013;154:283–93.
[24] François A, Schüetter N, Laffray S, Sanguesa J, Pizzoccaro A, Dubel S, Mantilleri A, Nargeot J, Noël J, Wood J, Moqrich A, Pongs O, Bourinet E. The low-threshold calcium channel $Ca_V3.2$ determines low-threshold mechanoreceptor function. Cell Rep 2015;10:370–82.
[25] Gabella G. The structural relations between nerve fibres and muscle cells in the urinary bladder of the rat. J Neurocytol 1995;24:159–87.
[26] García-Caballero A, Gadotti VM, Stemkowski P, Weiss N, Souza IA, Hodgkinson V, Bladen C, Chen L, Hamid J, Pizzoccaro A, Deage M, François A, Bourinet E, Zamponi GW. The deubiquitinating enzyme USP5 modulates neuropathic and inflammatory pain by enhancing $Ca_V3.2$ channel activity. Neuron 2014;83:1144–58.
[27] Geffeney SL, Goodman MB. How we feel: ion channel partnerships that detect mechanical inputs and give rise to touch and pain perception. Neuron 2012;74:609–19.
[28] Grundy L, Caldwell A, Brierley SM. Mechanisms underlying overactive bladder and interstitial cystitis/painful bladder syndrome. Front Neurosci 2018;12:931.
[29] Grundy L, Caldwell A, Garcia Caraballo S, Erickson A, Schober G, Castro J, Harrington AM, Brierley SM. Histamine induces peripheral and central hypersensitivity to bladder distension via the histamine H1 receptor and TRPV1. Am J Physiol Ren Physiol 2020;318:F298–314.
[30] Grundy L, Caldwell A, Garcia-Caraballo S, Grundy D, Spencer NJ, Dong X, Castro J, Harrington AM, Brierley SM. Activation of MrgprA3 and MrgprC11 on bladder-innervating afferents induces peripheral and central hypersensitivity to bladder distension. J Neurosci 2021;41: 3900–16.
[31] Grundy L, Caldwell A, Lumsden A, Mohammadi E, Hannig G, Greenwood Van-Meervald B, Brierley SM. Experimentally induced bladder permeability evokes bladder afferent hypersensitivity in the absence of inflammation. Front Neurosci 2020;14:590871.
[32] Grundy L, Chess-Williams R, Brierley SM, Mills K, Moore KH, Mansfield K, Rose'Meyer R, Sellers DJ, Grundy D. NKA enhances bladder afferent mechanosensitivity via urothelial and detrusor activation. Am J Physiol Ren Physiol 2018;315:F1174–85.
[33] Grundy L, Daly DM, Chapple C, Grundy D, Chess-Williams R. TRPV1 enhances the afferent response to P2X receptor activation in the mouse urinary bladder. Sci Rep 2018;8:197.
[34] Grundy L, Erickson A, Caldwell A, Garcia-Caraballo S, Rychkov G, Harrington A, Brierley SM. Tetrodotoxin-sensitive voltage-gated sodium

channels regulate bladder afferent responses to distension. PAIN 2018; 159:2573–84.
[35] Grundy L, Harrington AM, Caldwell A, Castro J, Staikopoulos V, Zagorodnyuk VP, Brookes SJH, Spencer NJ, Brierley SM. Translating peripheral bladder afferent mechanosensitivity to neuronal activation within the lumbosacral spinal cord of mice. PAIN 2019;160:793–804.
[36] Hanno PM. Interstitial cystitis-epidemiology, diagnostic criteria, clinical markers. Rev Urol 2002;4(suppl 1):S3–8.
[37] Hara K, Harris RA. The anesthetic mechanism of urethane: the effects on neurotransmitter-gated ion channels. Anesth Analgesia 2002;94: 313–18. table of contents.
[38] Heppenstall PA, Lewin GR. A role for T-type $Ca2^{+}$ channels in mechanosensation. Cell Calcium 2006;40:165–74.
[39] Heppner TJ, Tykocki NR, Hill-Eubanks D, Nelson MT. Transient contractions of urinary bladder smooth muscle are drivers of afferent nerve activity during filling. J Gen Physiol 2016;147:323–35.
[40] Hiramoto S, Tsubota M, Yamaguchi K, Okazaki K, Sakaegi A, Toriyama Y, Tanaka J, Sekiguchi F, Ishikura H, Wake H, Nishibori M, Nguyen HD, Okada T, Toyooka N, Kawabata A. Cystitis-Related bladder pain involves ATP-dependent HMGB1 release from macrophages and its downstream $H2S/Ca_v3.2$ signaling in mice. Cells 2020;9:1748.
[41] Hsu C-C, Liang C-C, Chang S-D, Chien C-W, Hsieh W-C. Comparison of urodynamic results and quality of life between women with interstitial cystitis and overactive bladder. Taiwan J Obstet Gynecol 2020;59:39–42.
[42] Igawa Y, Kumano S, Aizawa N, Saito Y, Ito H, Watanabe S, Takahashi N, Tajimi M, Nishimatsu H, Homma Y. Changes in the function and expression of T-type and N-type calcium channels in the rat bladder after bladder outlet obstruction. J Urol 2014;191:1159–67.
[43] Irwin DE, Milsom I, Hunskaar S, Reilly K, Kopp Z, Herschorn S, Coyne K, Kelleher C, Hampel C, Artibani W, Abrams P. Population-based survey of urinary incontinence, overactive bladder, and other lower urinary tract symptoms in five countries: results of the EPIC study. Eur Urol 2006;50: 1306–15. discussion 1314–1305.
[44] Jagodic MM, Pathirathna S, Joksovic PM, Lee W, Nelson MT, Naik AK, Su P, Jevtovic-Todorovic V, Todorovic SM. Upregulation of the T-type calcium current in small rat sensory neurons after chronic constrictive injury of the sciatic nerve. J Neurophysiol 2008;99:3151–6.
[45] Jarvis MF, Scott VE, McGaraughty S, Chu KL, Xu J, Niforatos W, Milicic I, Joshi S, Zhang Q, Xia Z. A peripherally acting, selective T-type calcium channel blocker, ABT-639, effectively reduces nociceptive and neuropathic pain in rats. Biochem Pharmacol 2014;89:536–44.
[46] Joksimovic SL, Joksimovic SM, Tesic V, García-Caballero A, Feseha S, Zamponi GW, Jevtovic-Todorovic V, Todorovic SM. Selective inhibition of Ca(V)3.2 channels reverses hyperexcitability of peripheral nociceptors and alleviates postsurgical pain. Sci Signal 2018;11:eaao4425.
[47] Kilkenny C, Browne WJ, Cuthill IC, Emerson M, Altman DG. Improving bioscience research reporting: the ARRIVE guidelines for reporting animal research. PLoS Biol 2010;8:e1000412.
[48] Knutson K, Alcaino C, Nayak V, Kacmaz H, Treichel AJ, Farrugia G, Beyder A. The T-type voltage gated calcium channel $Ca_v3.2$ is important for enteroendocrine cell mechanotransduction. FASEB J 2019;33:601.4.
[49] Konthapakdee N, Grundy L, O'Donnell T, Garcia-Caraballo S, Brierley SM, Grundy D, Daly DM. Serotonin exerts a direct modulatory role on bladder afferent firing in mice. J Physiol 2019;597:5247–64.
[50] Kraus RL, Li Y, Gregan Y, Gotter AL, Uebele VN, Fox SV, Doran SM, Barrow JC, Yang ZQ, Reger TS, Koblan KS, Renger JJ. In vitro characterization of T-type calcium channel antagonist TTA-A2 and in vivo effects on arousal in mice. J Pharmacol Exp Ther 2010;335:409–17.
[51] Liu Q, Sun B, Zhao J, Wang Q, An F, Hu X, Yang Z, Xu J, Tan M, Li L. Increased Piezo1 channel activity in interstitial Cajal-like cells induces bladder hyperactivity by functionally interacting with NCX1 in rats with cyclophosphamide-induced cystitis. Exp Mol Med 2018;50:1–16.
[52] Marger F, Gelot A, Alloui A, Matricon J, Ferrer JFS, Barrère C, Pizzoccaro A, Muller E, Nargeot J, Snutch TP, Eschalier A, Bourinet E, Ardid D. T-type calcium channels contribute to colonic hypersensitivity in a rat model of irritable bowel syndrome. Proc Natl Acad Sci U S A 2011;108:11268–73.
[53] Marshall KL, Saade D, Ghitani N, Coombs AM, Szczot M, Keller J, Ogata T, Daou I, Stowers LT, Bönnemann CG, Chesler AT, Patapoutian A. PIEZO2 in sensory neurons and urothelial cells coordinates urination. Nature 2020;588:290–5.
[54] Matsunami M, Miki T, Nishiura K, Hayashi Y, Okawa Y, Nishikawa H, Sekiguchi F, Kubo L, Ozaki T, Tsujiuchi T, Kawabata A. Involvement of the endogenous hydrogen sulfide/Ca(v) 3.2 T-type $Ca2^{+}$ channel pathway in cystitis-related bladder pain in mice. Br J Pharmacol 2012;167:917–28.
[55] Mills KA, West EJ, Grundy L, McDermott C, Sellers DJ, Rose'Myer RB, Chess-Williams R. Hypersensitivity of bladder low threshold, wide dynamic range, afferent fibres following treatment with the chemotherapeutic drugs cyclophosphamide and ifosfamide. Arch Toxicol 2020;94:2785–97.
[56] Ness TJ, Castroman PJ, Randich A. Acute bladder inflammation differentially affects rat spinal visceral nociceptive neurons. Neurosci Lett 2009;467:150–4.
[57] Ness TJ, DeWitte C, DeBerry JJ, Hart MP, Clodfelder-Miller B, Gu JG, Ling J, Randich A. A model in female rats with phenotypic features similar to interstitial cystitis/bladder pain syndrome. Front Pain Res 2021;2:2.
[58] Ness TJ, Elhefni H. Reliable visceromotor responses are evoked by noxious bladder distention in mice. J Urol 2004;171:1704–8.
[59] Ness TJ, Lewis-Sides A, Castroman P. Characterization of pressor and visceromotor reflex responses to bladder distention in rats: sources of variability and effect of analgesics. J Urol 2001;165:968–74.
[60] Ozaki T, Matsuoka J, Tsubota M, Tomita S, Sekiguchi F, Minami T, Kawabata A. Zinc deficiency promotes cystitis-related bladder pain by enhancing function and expression of $Ca_v3.2$ in mice. Toxicology 2018; 393:102–12.
[61] Perez-Reyes E. Molecular physiology of low-voltage-activated t-type calcium channels. Physiol Rev 2003;83:117–61.
[62] Picard E, Carvalho FA, Agosti F, Bourinet E, Ardid D, Eschalier A, Daulhac L, Mallet C. Inhibition of Ca(v) 3.2 calcium channels: a new target for colonic hypersensitivity associated with low-grade inflammation. Br J Pharmacol 2019;176:950–63.
[63] Proft J, Rzhepetskyy Y, Lazniewska J, Zhang FX, Cain SM, Snutch TP, Zamponi GW, Weiss N. The Cacna1h mutation in the GAERS model of absence epilepsy enhances T-type Ca(2+) currents by altering calnexin-dependent trafficking of $Ca_v3.2$ channels. Sci Rep 2017;7: 11513.
[64] Reger TS, Yang Z-Q, Schlegel K-AS, Shu Y, Mattern C, Cube R, Rittle KE, McGaughey GB, Hartman GD, Tang C, Ballard J, Kuo Y, Prueksaritanont T, Nuss CE, Doran SM, Fox SV, Garson SL, Li Y, Kraus RL, Uebele VN, Renger JJ, Barrow JC. Pyridyl amides as potent inhibitors of T-type calcium channels. Bioorg Med Chem Lett 2011;21:1692–6.
[65] Rong W, Spyer KM, Burnstock G. Activation and sensitisation of low and high threshold afferent fibres mediated by P2X receptors in the mouse urinary bladder. J Physiol 2002;541:591–600.
[66] Sadler KE, Stratton JM, Kolber BJ. Urinary bladder distention evoked visceromotor responses as a model for bladder pain in mice. J Vis Exp 2014;86:51413.
[67] Sekiguchi F, Kawabata A. T-type calcium channels: functional regulation and implication in pain signaling. J Pharmacol Sci 2013;122:244–50.
[68] Shin JB, Martinez-Salgado C, Heppenstall PA, Lewin GR. A T-type calcium channel required for normal function of a mammalian mechanoreceptor. Nat Neurosci 2003;6:724–30.
[69] Spencer NJ, Greenheigh S, Kyloh M, Hibberd TJ, Sharma H, Grundy L, Brierley SM, Harrington AM, Beckett EA, Brookes SJ, Zagorodnyuk VP. Identifying unique subtypes of spinal afferent nerve endings within the urinary bladder of mice. J Comp Neurol 2018;526:707–20.
[70] Stewart WF, Van Rooyen JB, Cundiff GW, Abrams P, Herzog AR, Corey R, Hunt TL, Wein AJ. Prevalence and burden of overactive bladder in the United States. World J Urol 2003;20:327–36.
[71] Sui GP, Wu C, Fry CH. Inward calcium currents in cultured and freshly isolated detrusor muscle cells: evidence of a t-type calcium current. J Urol 2001;165:621–6.
[72] Suskind AM, Berry SH, Suttorp MJ, Elliott MN, Hays RD, Ewing BA, Clemens JQ. Health-related quality of life in patients with interstitial cystitis/bladder pain syndrome and frequently associated comorbidities. Qual Life Res 2013;22:1537–41.
[73] Takahashi T, Aoki Y, Okubo K, Maeda Y, Sekiguchi F, Mitani K, Nishikawa H, Kawabata A. Upregulation of $Ca_v3.2$ T-type calcium channels targeted by endogenous hydrogen sulfide contributes to maintenance of neuropathic pain. PAIN 2010;150:183–91.
[74] To KHT, Gui P, Li M, Zawieja SD, Castorena-Gonzalez JA, Davis MJ. T-type, but not L-type, voltage-gated calcium channels are dispensable for lymphatic pacemaking and spontaneous contractions. Sci Rep 2020;10: 70.
[75] Usoskin D, Furlan A, Islam S, Abdo H, Lönnerberg P, Lou D, Hjerling-Leffler J, Haeggström J, Kharchenko O, Kharchenko PV, Linnarsson S, Ernfors P. Unbiased classification of sensory neuron types by large-scale single-cell RNA sequencing. Nat Neurosci 2015;18:145–53.
[76] Vanneste M, Segal A, Voets T, Everaerts W. Transient receptor potential channels in sensory mechanisms of the lower urinary tract. Nat Rev Urol 2021;18:139–59.
[77] Vlaskovska M, Kasakov L, Rong W, Bodin P, Bardini M, Cockayne DA, Ford APDW, Burnstock G. P2X3 knock-out mice reveal a major sensory role for urothelially released ATP. J Neurosci 2001;21:5670–7.
[78] Wang R, Lewin GR. The $Ca_v3.2$ T-type calcium channel regulates temporal coding in mouse mechanoreceptors. J Physiol 2011;589:2229–43.

[79] Wu J, Peng S, Xiao L, Cheng X, Kuang H, Zhu M, Zhang D, Jiang C, Liu T. Cell-type specific distribution of T-type calcium currents in lamina II neurons of the rat spinal cord. Front Cell Neurosci 2018;12:370.
[80] Yanai Y, Hashitani H, Kubota Y, Sasaki S, Kohri K, Suzuki H. The role of Ni(2+)-sensitive T-type Ca(2+) channels in the regulation of spontaneous excitation in detrusor smooth muscles of the Guinea-pig bladder. BJU Int 2006;97:182–9.
[81] Yoshiyama M, Mochizuki T, Nakagomi H, Miyamoto T, Kira S, Mizumachi R, Sokabe T, Takayama Y, Tominaga M, Takeda M. Functional roles of TRPV1 and TRPV4 in control of lower urinary tract activity: dual analysis of behavior and reflex during the micturition cycle. Am J Physiol Ren Physiol 2015;308:F1128–1134.
[82] Zagorodnyuk VP, Brookes SJH, Spencer NJ, Gregory S. Mechanotransduction and chemosensitivity of two major classes of bladder afferents with endings in the vicinity to the urothelium. J Physiol 2009;587:3523–38.
[83] Zagorodnyuk VP, Gibbins IL, Costa M, Brookes SJH, Gregory SJ. Properties of the major classes of mechanoreceptors in the Guinea pig bladder. J Physiol 2007;585:147–63.
[84] Zamponi GW, Striessnig J, Koschak A, Dolphin AC. The physiology, pathology, and pharmacology of voltage-gated calcium channels and their future therapeutic potential. Pharmacol Rev 2015;67:821–70.
[85] Zeisel A, Hochgerner H, Lönnerberg P, Johnsson A, Memic F, van der Zwan J, Häring M, Braun E, Borm LE, La Manno G, Codeluppi S, Furlan A, Lee K, Skene N, Harris KD, Hjerling-Leffler J, Arenas E, Ernfors P, Marklund U, Linnarsson S. Molecular architecture of the mouse nervous System. Cell 2018;174:999–1014.e22.